


Id2 controls specification of Lgr5⁺ intestinal stem cell progenitors during gut development

Lira Nigmatullina, Maxim Norkin, Margarita M Dzama, Berith Messner, Sergi Sayols & Natalia Soshnikova* 

Abstract

The adult intestinal stem cells (ISCs), their hierarchies, mechanisms of maintenance and differentiation have been extensively studied. However, when and how ISCs are established during embryogenesis remains unknown. We show here that the transcription regulator Id2 controls the specification of embryonic Lgr5⁺ progenitors in the developing murine small intestine. Cell fate mapping analysis revealed that Lgr5⁺ progenitors emerge at E13.5 in wild-type embryos and differ from the rest on the intestinal epithelium by a characteristic ISC signature. In the absence of Id2, the intestinal epithelium differentiates into Lgr5⁺ cells already at E9.5. Furthermore, the size of the Lgr5⁺ cell pool is significantly increased. We show that Id2 restricts the activity of the Wnt signalling pathway at early stages and prevents precocious differentiation of the embryonic intestinal epithelium. Id2-deficient embryonic epithelial cells cultured *ex vivo* strongly activate Wnt target genes as well as markers of neoplastic transformation and form fast growing undifferentiated spheroids. Furthermore, adult ISCs from Id2-deficient mice display a distinct transcriptional signature, supporting an essential role for Id2 in the correct specification of ISCs.

Keywords epithelial neoplasia; intestinal organoids; ISC transcriptional signature; small intestine; Wnt signalling

Subject Categories Development & Differentiation; Stem Cells

DOI 10.15252/embj.201694959 | Received 6 June 2016 | Revised 8 December 2016 | Accepted 9 December 2016 | Published online 11 January 2017

The EMBO Journal (2017) 36: 869–885

See also: **K Kretzschmar & H Clevers** (April 2017)

Introduction

The adult small intestinal epithelium is composed of two compartments: differentiated villi and proliferating crypts. Continuous renewal of the adult intestinal tissue is supported by intestinal stem cells (ISCs) positioned at the bottom of the crypts. The adult ISCs divide to generate stem cells and transit amplifying daughter cells, which further give rise to various terminally differentiated progenies: absorptive enterocytes, secretory goblet, entero-endocrine, tuft

and Paneth cells (Clevers *et al*, 2014). Genetic studies have defined Wnt signalling as a crucial regulator of the adult ISCs proliferation, maintenance and differentiation (Clevers *et al*, 2014). Loss-of-function mutations in negative regulators of Wnt signalling (Shibata *et al*, 1997) or ectopic expression of Wnt agonists (Kim *et al*, 2005) lead to hyperplasia of intestinal crypts. On the other hand, ablation of *Tcf7l2* or β -catenin, encoding downstream effectors of the Wnt pathway, causes loss of crypts formation (Korinek *et al*, 1998; Fevr *et al*, 2007; Chin *et al*, 2016). Gene expression and lineage tracing studies revealed multiple markers of the adult ISCs, such as *Lgr5* (Barker *et al*, 2007), *Ascl2* (van der Flier *et al*, 2009a), *Olfm4* (van der Flier *et al*, 2009b), *Smoc2* (Muñoz *et al*, 2012) and *Lrig1* (Powell *et al*, 2012; Wong *et al*, 2012), many of which are targets and mediators of Wnt signalling (Clevers *et al*, 2014). In contrast to our good understanding of Wnt-dependent transcriptional programmes operating in the adult ISCs, it remains unclear what is the importance of Wnt signalling during development of the embryonic small intestinal epithelium.

In mice, the primitive gut tube is formed by embryonic day 9 (E9.0) (Wells & Spence, 2014). It remains as a simple tube comprised of morphologically identical highly proliferative epithelial cells surrounded by layers of mesenchyme till E14.5, a time point when the gut epithelium begins to differentiate. At late foetal stages, between E15.5 and E18.5, the embryonic epithelium forms villi and inter-villi (future crypts). Several studies have demonstrated that cells expressing the adult ISC markers, including *Lgr5*, *Ascl2* and *Olfm4*, appear at E15.5 within the inter-villus regions (Korinek *et al*, 1998; Garcia *et al*, 2009; Kinzel *et al*, 2014), suggesting that Wnt-dependent progenitors of the adult ISCs are established at this developmental stage, which is consistent with phenotypes displayed by *Tcf7l2* or β -catenin mutant mice (Korinek *et al*, 1998; Chin *et al*, 2016). However, there was a conflicting report describing ubiquitous expression of *Lgr5* in the embryonic intestinal epithelium already at E12.5 (Shyer *et al*, 2015) and proposing that the early gut epithelium consists of a uniform pool of Wnt-dependent progenitors. This discrepancy has raised important questions about the time of the intestinal epithelial progenitor specification as well as functional and molecular homogeneity of the early embryonic small intestinal epithelium.

Another question is how the ISCs programme is regulated during development. The basic helix-loop-helix (bHLH) transcription factor

Ascl2 is specifically expressed in the adult ISCs (van der Flier *et al*, 2009a) and cooperates with Tcf7l2 to activate a set of stem cell genes (Schuijers *et al*, 2015). However, in the embryonic small intestine, *Ascl2* was shown to be expressed only after E15.5 (van der Flier *et al*, 2009a; Garcia *et al*, 2009) and its functions in the developing intestine remain unknown. The zinc-finger transcription factor Gata6, in concert with Tcf7l2, positively regulates the expression of a subset of Wnt-dependent genes in colorectal cancer (Whissell *et al*, 2014). In contrast, loss of both *Gata6* and *Gata4* in embryonic small intestine results in activation of ISCs markers, such as *Lgr5* and *Cd44* at E16.5 (Walker *et al*, 2014). Bmp signalling and its mediators, Smad and Id transcription factors, negatively control self-renewal of the adult ISCs and attenuate intestinal tumour formation (Takaku *et al*, 1998; Haramis *et al*, 2004; He *et al*, 2004; Russell *et al*, 2004; Sodik *et al*, 2006). Yet, their functions in the regulation of intestinal stem cells during embryonic development remain unknown.

In the present study, using lineage tracing analysis, we demonstrate that a small population of embryonic Lgr5⁺ progenitors emerges during late intestinal development, after E13.5. Transcriptome profiling showed that the embryonic Lgr5⁺ cells have a unique molecular signature. We found that Id2 controls the timing of Lgr5⁺ cells specification. We show that at the molecular level, Id2 prevents precocious maturation of the early embryonic epithelium and restricts the number of Lgr5⁺ progenitors by inhibiting early activation of Wnt signalling. Precocious Lgr5⁺ cells show distinct growth properties *ex vivo* and ultimately give rise, *in vivo*, to adult ISCs with an altered transcriptional programme.

Results

Embryonic intestinal epithelium and adult ISCs have distinct molecular signatures

To gain insight into the molecular properties of mouse embryonic intestinal epithelium, we performed whole-transcriptome RNA-sequencing of EpCAM-positive epithelial cells (Fig 1A) isolated by flow cytometry from dissected small intestines at E11.5 (Fig 1B and Appendix Fig S1A), the earliest time point when the small intestine is clearly demarcated from stomach and large intestine. Approximately one thousand EpCAM⁺ cells could be obtained from one embryo at this stage of development. We have also

sequenced the transcriptomes of Lgr5-EGFP^{high} adult ISCs (Fig 1C; Barker *et al*, 2007) purified by FACS from the small intestines of 2-month-old (P60) Lgr5^{EGFP-Cre-ERT} mice (Fig 1D and Appendix Fig S1B; Barker *et al*, 2007). Comparative analyses of the embryonic and adult transcriptomes revealed over 4,500 differentially expressed genes (log₂FC ≥ 1, FDR < 0.01, Fig 1E and Datasets EV1 and EV2), which represent almost half of the total transcriptome, indicating that very distinct transcriptional programmes operate in the embryonic and adult intestinal epithelium. Gene ontology analysis of the transcripts expressed at over 50 times higher levels in the embryonic epithelium showed the highest enrichment scores for signal peptide and secreted protein categories (147 and 88 out of 466 genes, respectively, Fig 1F). In contrast, genes upregulated 2–10 times were associated with RNA splicing, chromatin and transcriptional regulation pathways (Fig 1F). This included transcription factors *Foxa2*, *Sall4*, *Satb1*, *Sox11*, *Tcf7l1* and *Prdm1* as well as chromatin interacting proteins *Asf1a*, *Cbx2*, *Cbx4*, *Dnmt3a*, *Smarcd3*, *Suv39h2* and *Suv420h2*. In the adult ISCs, the largest groups of genes upregulated over 50 times belong to antimicrobial defence and signal peptide categories (31 and 92 out of 305 genes, respectively, Fig 1F). Furthermore, genes upregulated 2–10 times in the adult ISCs were enriched for mitochondrion and ribosomal functions (203 and 44 out of 1,771 genes, respectively, Fig 1F), which is consistent with distinct cellular and metabolic processes in the embryonic and adult gut.

We found that multiple genes regulating various signalling pathways were expressed at higher levels in the embryonic epithelium, such as members of Hedgehog signalling (*Ihh*, *Shh*, *Gas1*, *Sufu* and *Gli3*), TGFβ/Bmp signalling (*BMP* and *activin membrane-bound inhibitor homolog (Bambi)*, *Bmp1*, *Bmpr1b*, *Tgfb3*, *Smad6* and *Smad7*), FGF signalling (*Fgf9*, *Fgfr1*, *Fgfr2* and *Fgfr4*) and IGF signalling (*Igf2*, *Igf2bp1*, *Igf2bp3*, *Igfbp2*, *Igfbp5*, *Igfbp7* and *H19*) (Appendix Fig S1C–E). Quantitative reverse transcription-PCR (qRT-PCR) and *in situ* hybridization analyses further confirmed RNA-sequencing data (Fig 1G–Z). Interestingly, several negative regulators of the Wnt pathway, including *Sfrp1*, *Sfrp2*, *Sfrp5*, *Robo1/2*, *Shisa6*, *Glis2*, *Tcf7l1* and *Ctnnbip1*, were transcribed at higher levels in the embryonic intestinal epithelium compared to the adult ISCs (Fig 1L–P). Accordingly, well-known targets of Wnt signalling expressed in the adult ISCs (Muñoz *et al*, 2012), such as *Lgr5*, *Ascl2*, *Axin2*, *Cd44*, *Slc12a2* and *Smoc2*, were either absent or barely detectable in the embryonic intestinal epithelial cells (Fig 1Q–Z and

Figure 1. Molecular signature of embryonic intestinal epithelium.

- A Confocal image of the embryonic small intestine at E11.5. EpCAM (orange) specifically labels epithelial cells. DAPI staining (blue) shows nuclei.
- B Representative fluorescence-activated cell sorting (FACS) plot showing EpCAM⁺ embryonic epithelial small intestinal cells (orange) at E11.5 (*n* = 6).
- C Lgr5-EGFP-expressing adult ISCs (green) are at the base of a crypt.
- D Representative FACS plot showing Lgr5-EGFP^{high} adult ISCs (green) (*n* = 6).
- E Analysis of RNA-seq data showing the number of differentially expressed genes between embryonic small intestinal epithelium at E11.5 and the adult ISCs.
- F GO analysis displaying the significantly enriched molecular functions in the groups of upregulated genes in embryonic small intestinal epithelium (orange) and the adult ISCs (green).
- G–Z (G, L, Q, V) UCSC Genome Browser images of RNA-seq data, with transcript profiles of polyA⁺ mRNA from embryonic small intestinal epithelium (orange) and the adult ISCs (green). *Shh* and *Sfrp5* are highly expressed in the embryonic small intestine (G, L), whereas *Lgr5* and *Axin2* were detected in the adult ISCs only (Q, V). The y-axis indicates the coverage normalized by library size (reads per million). qRT-PCR analysis for *Shh* (H), *Sfrp5* (M), *Lgr5* (R) and *Axin2* (W) in embryonic (orange) and the adult ISCs (green) cells. *Epcam* expression was used as normalizing control. Error bars are ± SD, *n* = 3. ***P* < 0.01 by Student's *t*-test. RNA *in situ* hybridization analysis showing the expression of *Shh* (I), *Sfrp5* (N), *Lgr5* (S) and *Axin2* (X) in the embryonic small intestine at E11.5. Expression of *Shh* (J, K), *Sfrp5* (O, P), *Lgr5* (T, U) and *Axin2* (Y, Z) in the adult small intestine.

Data information: Scale bar: 27 μm (A), 100 μm (C), 20 μm (I, N, S, X), 50 μm (J, O, T, Y) and 11 μm (K, P, U, Z). See also Appendix Fig S1.

Appendix Fig S1F and G). The same was true for the other intestinal stem cell markers, such as *Olfm4* and *Lrig1* (Appendix Fig S1H). These results demonstrate that although the embryonic intestinal epithelium and the adult ISCs share the molecular signature of endodermal lineage, the intestinal stem cell signature is absent in the embryonic gut at E11.5.

Lgr5⁺ cells represent a small fraction of the embryonic gut epithelium and define late embryonic progenitors of the adult ISCs

Our RNA-sequencing and RNA *in situ* hybridization analyses did not support the conclusions of a study reporting that the adult ISC

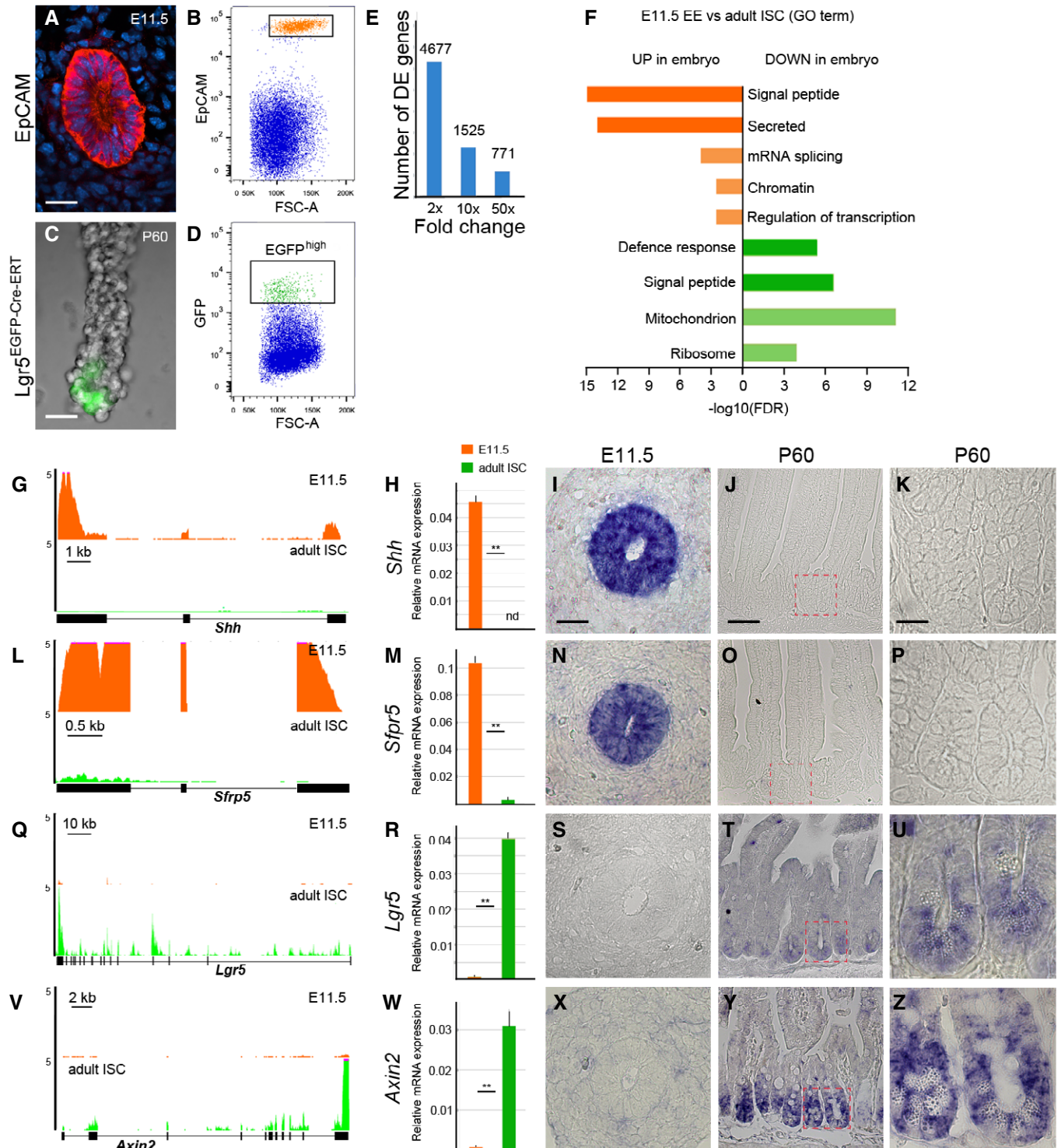


Figure 1.

markers, *Lgr5* and *Cd44*, are expressed throughout the embryonic intestinal epithelium (Shyer *et al*, 2015). Therefore, we re-evaluated *Lgr5* expression in the intestinal epithelium of *Lgr5*^{EGFP-Cre-ERT} embryos at different developmental stages. Using FACS analysis, we detected $0.66 \pm 0.1\%$ of Lgr5-EGFP⁺ cells in the embryonic small intestine at E12.5 (Figs 2A and EV1A and B). The number of Lgr5-EGFP⁺ cells increased progressively during development, from $7.4 \pm 2.2\%$ at E13.5 to $17.1 \pm 2.5\%$ at E17.5 (Figs 2A and EV1C–H). Accordingly, both RNA *in situ* hybridization and immunostaining for EGFP confirmed that *Lgr5* was expressed only in a subset of intestinal epithelial cells at E12.5 and E13.5 (Figs 2B and EV1I–P). A higher number of Lgr5⁺ cells was observed in the posterior compared to the anterior small intestine at all embryonic stages analysed (see also below). Moreover, Lgr5-EGFP⁺ cells were mostly detected in a specific domain, close to the caecum, of the small intestine at E12.5 (Fig EV1M).

We assessed the contribution of embryonic Lgr5-EGFP⁺ cells to the adult small intestine by lineage tracing analysis using *Lgr5*^{EGFP-Cre-ERT} and *Rosa26*^{LacZ} reporter mice. A single tamoxifen administration to *Lgr5*^{EGFP-Cre-ERT}/*Rosa26*^{LacZ} mice at E13.5 gave few LacZ⁺ clones (14 ± 4 , $n = 3$) after a 2 months chase (P60, Fig 2C). Consistent with the increasing number of *Lgr5*-expressing cells during development, the amount of LacZ⁺ clones within the adult small intestine also increased upon tamoxifen induction at E14.5 (127 ± 15 , $n = 3$) and E15.5 (186 ± 22 , $n = 3$) (Fig 2D and E). Moreover, to test whether the amount of LacZ⁺ cells could reflect

the low recombination efficiency of the *Rosa26*^{LacZ} reporter line, we used the very efficient *Rosa26*^{tdTomato} reporter. The numbers of Lgr5⁺:tdTomato⁺ cells were quantified by FACS 1 day after tamoxifen induction using *Lgr5*^{EGFP-Cre-ERT}/*Rosa26*^{tdTomato} embryos at different developmental stages (Fig 2F and Appendix Fig S2A–C). Of note, we have not detected unspecific labelling in the absence of either tamoxifen or Cre-ERT, using both reporter lines. The low number of LacZ⁺ clones in the adult tissue was in accordance with the low percentage of tdTomato⁺ cells observed in embryos. For example, only $1.9 \pm 0.5\%$ of Lgr5-EGFP⁺:tdTomato⁺ cells were detected after labelling at E15.5 (Fig 2A and F). In contrast, a single dose of tamoxifen administered to *Rosa26*^{Cre-ERT}/*Rosa26*^{tdTomato} mice at E13.5 resulted in $98.6 \pm 1.1\%$ of labelled cells (Appendix Fig S2D–G). These results indicate that *Lgr5*-Cre-ERT is expressed at very low levels during embryogenesis. Further immuno-histological analyses showed that Lgr5⁺ progenies gave rise to all differentiated intestinal epithelial cell types, including enterocytes, chromogranin A-positive entero-endocrine, goblet and Paneth cells (Fig 2G–I). Taken together, our data demonstrate that embryonic Lgr5⁺ cells contribute to the pool of adult ISCs after E13.5.

Molecular signature of embryonic Lgr5⁺ progenitors

To define how similar Lgr5⁺ embryonic progenitors are to the adult ISCs and possibly identify factors regulating their specification during embryogenesis, we sequenced the transcriptomes of

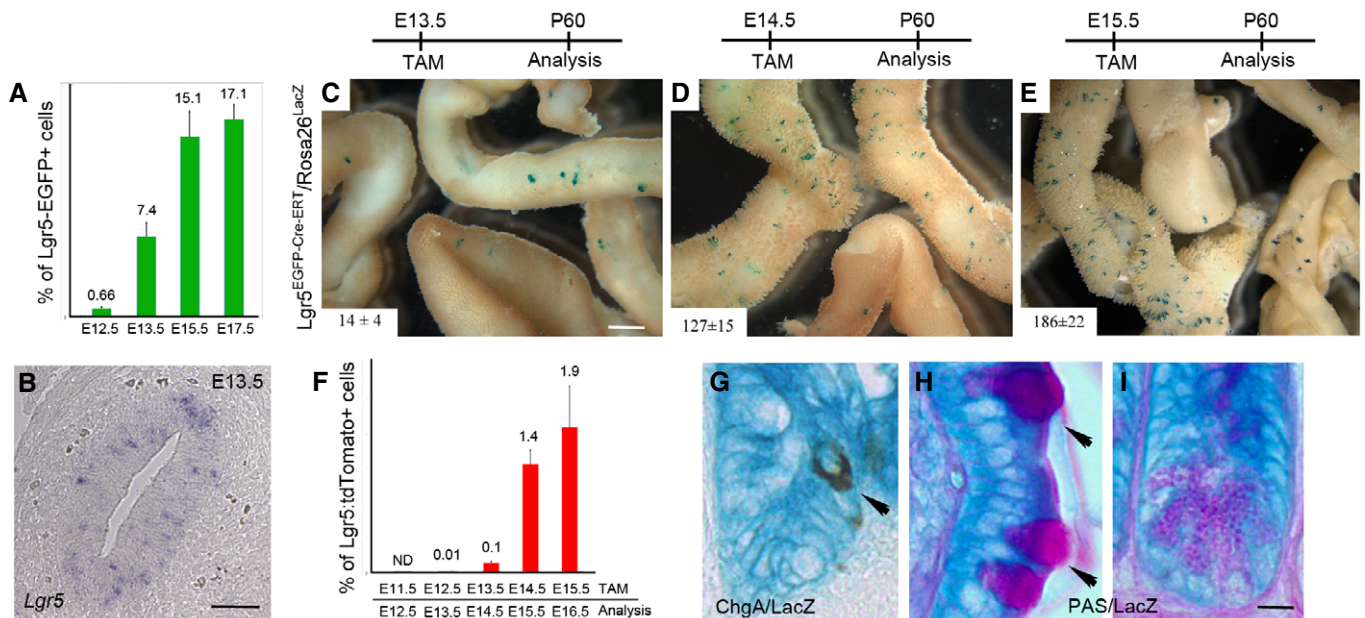


Figure 2. Fate mapping of embryonic Lgr5⁺ cells.

- A Quantitative FACS analysis of Lgr5-EGFP⁺ cells in small intestinal epithelium of *Lgr5*^{EGFP-Cre-ERT} embryos at various developmental stages. Error bars are \pm SD, $n \geq 3$.
 B Expression pattern of *Lgr5* in the embryonic small intestine at E13.5.
 C–E Whole-mount view of LacZ-stained *Lgr5*^{EGFP-Cre-ERT}/*Rosa26*^{LacZ} small intestines 2 months (P60) after a single treatment with TAM at E13.5 (C), E14.5 (D) and E15.5 (E) ($n = 3$). The number of LacZ⁺ clones is indicated for each stage.
 F Quantitative FACS analysis of Lgr5-EGFP⁺:tdTomato⁺EpCAM⁺ cells 1 day after a single treatment with TAM at different embryonic stages. Error bars are \pm SD, $n > 3$.
 G Immuno-labelling for chromogranin A (ChgA) reveals entero-endocrine cells (brown, arrowhead) surrounded by enterocytes within LacZ⁺ (blue) villi.
 H, I Co-staining with PAS shows goblet (pink, arrowheads, H) and Paneth cells (pink granules, I) positive for LacZ activity (blue).

Data information: Scale bar: 30 μ m (B), 1.5 mm (C–E) and 4.5 μ m (G–I). See also Fig EV1 and Appendix Fig S2.

FACS-purified Lgr5-EGFP⁺EpCAM⁺ and corresponding control Lgr5-EGFP⁻EpCAM⁺ cells from the embryonic small intestines at E13.5 (Fig 3A and Appendix Fig S3A and B), the earliest time point when 200–500 Lgr5⁺EpCAM⁺ cells are present within the embryonic intestinal epithelium. Comparative analysis revealed 500 differentially expressed genes between Lgr5⁺EpCAM⁺ and control cells ($\log_2FC \geq 0.5$, FDR < 0.01, Fig 3B and Datasets EV3 and EV4). The changes in gene expression were moderate, maximum fivefold, with 50% of genes being less than twofold differentially expressed. The differential expression of genes identified by RNA-sequencing was further confirmed by qRT-PCR analysis (Fig 3C). Gene Ontology analysis revealed that the embryonic Lgr5⁺ transcriptome was enriched for the genes promoting cell cycle progression and proliferation (31 out of 247 genes, $P < 10^{-20}$) compared to the control Lgr5⁻EpCAM⁺ cells. The gene list includes *Aurka*, *Aurkb*, *Cyclin-dependent kinase 1 (Cdk1)*, *Cyclin a2*, *Cyclin b2*, *Cdc25* and *Plk1*. Out of 247 embryonic Lgr5⁺ signature genes, 36 (14.6%, $P < 10^{-15}$) overlapped with the adult ISCs signature (Fig 3D) and included key ISCs markers (Muñoz *et al*, 2012), such as *Ascl2*, *Axin2*, *CD44*, *Kcne3*, *Slc12a2*, *Smoc2* and *Tnfrsf19* (Fig 3B, C, E and F, and Dataset EV3). Further analysis revealed that the expression of those genes was fourfold to 15-fold lower in embryos compared to the adult ISCs (Appendix Fig S3C and D), suggesting that the embryonic Lgr5⁺ cells undergo a maturation process to develop their full stem cell potential. Consistently, several ISCs markers, including *Lrig1*, *Prom1*, *Rnf43* and *Olfm4*, were absent or expressed at too low levels and were not identified as differentially expressed in embryonic gut (Appendix Fig S3E–H).

Of the 260 genes downregulated in Lgr5⁺EpCAM⁺ cells, the largest group belongs to glycoproteins and lipid and fatty acid transport proteins as determined by GO analysis (3.2-fold enrichment, $P < 10^{-4}$). Known markers of differentiated intestinal epithelium, including *Fabp1*, *Fabp2*, *Anpep*, *Afp*, *Rbp2* and *Rbp4*, were found to be the most strongly downregulated (Dataset EV4). *Sfrp5*, *Onecut2* and *Gata4*, which are essential for proper differentiation of the embryonic intestinal epithelium (Matsuyama *et al*, 2009; Dusing *et al*, 2010; Kohlnhofer *et al*, 2016), were between a few signalling molecules or transcription factors decreased in Lgr5⁺ cells (Fig 3C, G–H). In summary, our data demonstrate that the transcriptional changes leading to the ISCs specification take place during late embryogenesis, around E13.5. This regulatory shift consists of both upregulation of the Wnt signalling responsive genes and repression of genes mediating metabolic functions of differentiated gut epithelium.

***Id2* controls timing of Lgr5⁺ cell specification in the embryonic intestinal epithelium**

To identify factors involved in a correct specification of Lgr5⁺ progenitors, we focused on genes (i) highly expressed in the embryonic intestinal epithelium at E11.5 and absent in the adult ISCs, and (ii) regulating either the expression or function of key factors controlling the adult ISCs programme, such as *Ascl2*, β -catenin and *Tcf7l2*. We have selected *Id2*, encoding a transcriptional regulator containing a HLH domain (Lasorella *et al*, 2014), which was highly expressed in the embryonic gut at E11.5 (Fig 4A–E). *Id2* promotes differentiation and suppresses tumour formation in the intestinal epithelium (Fig EV2A–D and Russell *et al*, 2004). However, what

happens at the molecular level in *Id2* mutant intestinal epithelium is not known. To explore the functions of *Id2* in the embryonic gut, we have used *Id2*^{Cre-ERT} knock-in mice, in which the *Id2* gene is replaced by a *Cre-ERT* cassette thus representing a null allele of *Id2* (Rawlins *et al*, 2009).

We assessed the consequences of *Id2* inactivation on Lgr5 expression in *Id2*^{Cre-ERT/Cre-ERT}:Lgr5^{EGFP-Cre-ERT} (further referred to as *Id2KO*:Lgr5^{EGFP-Cre-ERT}) mutant embryos at different developmental stages using both immunostaining and FACS analyses. Importantly, *Id2* deletion resulted in ectopic, precocious activation of Lgr5-EGFP in the intestinal epithelium of mutant embryos already at E9.5 as revealed by immunostaining for GFP (Fig 4F and G). At E11.5, Lgr5⁺ cells were mostly found in the posterior half of the small intestine in *Id2KO*:Lgr5^{EGFP-Cre-ERT} embryos (Figs 4H and I, and EV2E and F). FACS analysis further determined that 36.4 ± 5.4% (56-fold, $P < 10^{-7}$) of embryonic intestinal epithelial cells were Lgr5⁺ in *Id2* mutants at E11.5 (Figs 4J and EV2G and H). This ectopic activation was also detected in *Id2* heterozygous embryos, although to a lesser extent, 5.3 ± 1.9% (eightfold, $P = 1.5 \times 10^{-4}$) (Fig 4J). At E15.5, when the embryonic intestinal epithelium begins to divide into Lgr5⁺ inter-villi and Lgr5⁻ villi compartments, 64 ± 8.5% (6.4-fold, $P < 10^{-5}$) and 90 ± 2.7% (2.1-fold, $P < 10^{-5}$) of epithelial cells were Lgr5⁺ in the anterior and posterior halves of the small intestine in *Id2KO*:Lgr5^{EGFP-Cre-ERT} embryos, respectively (Fig 4J).

Interestingly, Lgr5-EGFP⁺ cells were observed in both villi and inter-villi compartments in the posterior intestine of *Id2KO* embryos (Fig 4K and L). By E17.5, when cyto-differentiation of the embryonic intestinal epithelium is completed, the number of Lgr5⁺ cells was only slightly elevated (1.2-fold, $P < 0.05$) in the anterior small intestine of the mutant embryos compared to wild type (Fig 4J). In contrast, significantly more (2.4-fold, $P < 10^{-6}$) Lgr5⁺ cells were detected in the posterior half of the mutant intestine at this stage (Fig 4J). At this time point, similar to the wild-type situation, Lgr5⁺ cells were detected only in the inter-villi compartment in *Id2KO* (Fig 4M and N). Yet, the number of bright GFP⁺ cells was higher in *Id2KO* compared to wild type. These data demonstrate that *Id2* negatively regulates the initiation of Lgr5⁺ cell specification as well as their numbers in the small intestinal epithelium during development.

Effect of *Id2* loss on the embryonic intestinal epithelium transcriptome

To determine the molecular signature of Lgr5⁺EpCAM⁺ cells in *Id2KO*:Lgr5^{EGFP-Cre-ERT} intestinal epithelium at E11.5, we isolated 250 Lgr5⁺EpCAM⁺, Lgr5⁻EpCAM⁺ and control (from Lgr5^{EGFP-Cre-ERT} embryos) Lgr5⁻EpCAM⁺ cells by FACS and performed RNA-sequencing analyses (Fig EV2G and H). We found over 800 genes differentially expressed between *Id2KO*Lgr5⁺EpCAM⁺ and *Id2KO*Lgr5⁻EpCAM⁺ cells ($\log_2FC \geq 0.5$, FDR < 0.01, Datasets EV5 and EV6). An even higher number of differentially expressed genes were detected between *Id2KO*Lgr5⁺EpCAM⁺ and control Lgr5⁻EpCAM⁺ cells (over 900 genes, Fig 5A and C, and Datasets EV7 and EV8), whereas changes in the expression of only 338 genes were found between *Id2KO*Lgr5⁻EpCAM⁺ and control Lgr5⁻EpCAM⁺ (Fig 5A and C, and Datasets EV9 and EV10).

Transcriptome profiling confirmed by qRT-PCR showed that *Id2* negatively regulates the expression of approximately 600 genes in

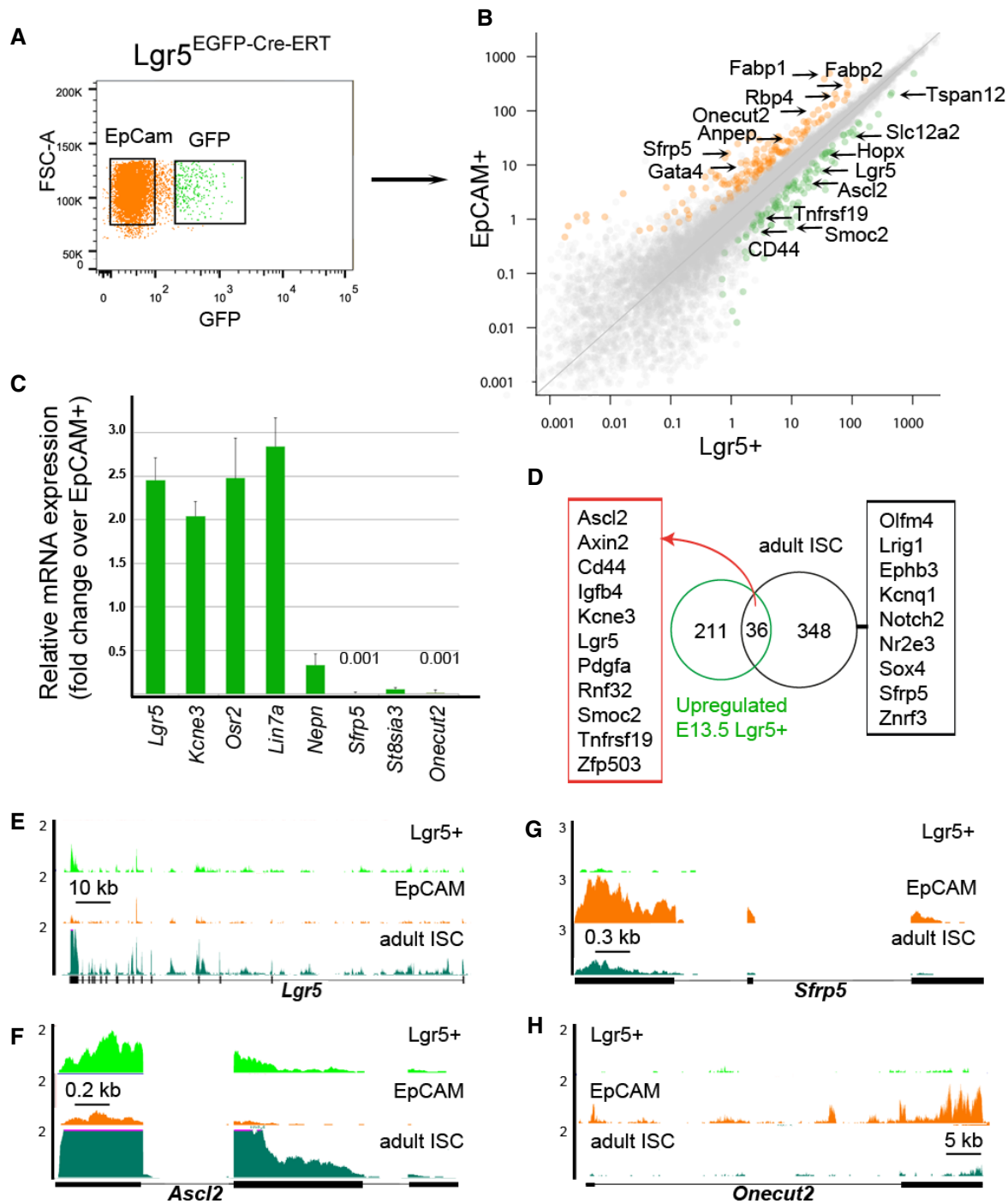


Figure 3. Transcriptional signature of embryonic Lgr5⁺ cells.

A A representative FACS plot showing strategy to isolate Lgr5-EGFP⁺EpCAM⁺ (green), and control Lgr5-EGFP⁻EpCAM⁺ cells (orange) for RNA-seq analysis at E13.5 ($n \geq 10$).

B RPKM scatter plot illustrating gene expression profiles of Lgr5⁺ (x-axis) and EpCAM⁺ (y-axis) cells. Genes significantly upregulated in Lgr5⁺ compared to EpCAM⁺ cells ($\log_2FC \geq 1$, FDR < 0.01) are in green. Genes significantly upregulated in EpCAM⁺ compared to Lgr5⁺ cells ($\log_2FC \geq 1$, FDR < 0.01) are in orange.

C qRT-PCR analysis for selected genes differentially expressed in Lgr5⁺ compared to control EpCAM⁺ cells. Relative expression levels of each gene in EpCAM⁺ were fixed to 1. *EpCam* expression was used as normalizing control. Error bars are \pm SD, $n = 4$.

D Venn diagram showing the overlap between genes upregulated in the embryonic Lgr5⁺ cells and the adult ISCs signature.

E-H UCSC Genome Browser images of RNA-seq data, with transcript profiles of mRNA from embryonic Lgr5⁺ (green), EpCAM⁺ cells (orange) at E13.5 and the adult ISCs (teal) ($n = 4$). *Lgr5* (E) and *Ascl2* (F) are upregulated in the embryonic Lgr5⁺ cells and are highly expressed in the adult ISCs. In contrast, *Sfrp5* (G) and *Onecut2* (H) are expressed at higher levels in the Lgr5⁻ EpCAM⁺ cells. The y-axis indicates the coverage normalized by library size (reads per million).

Data information: See also Appendix Fig S3.

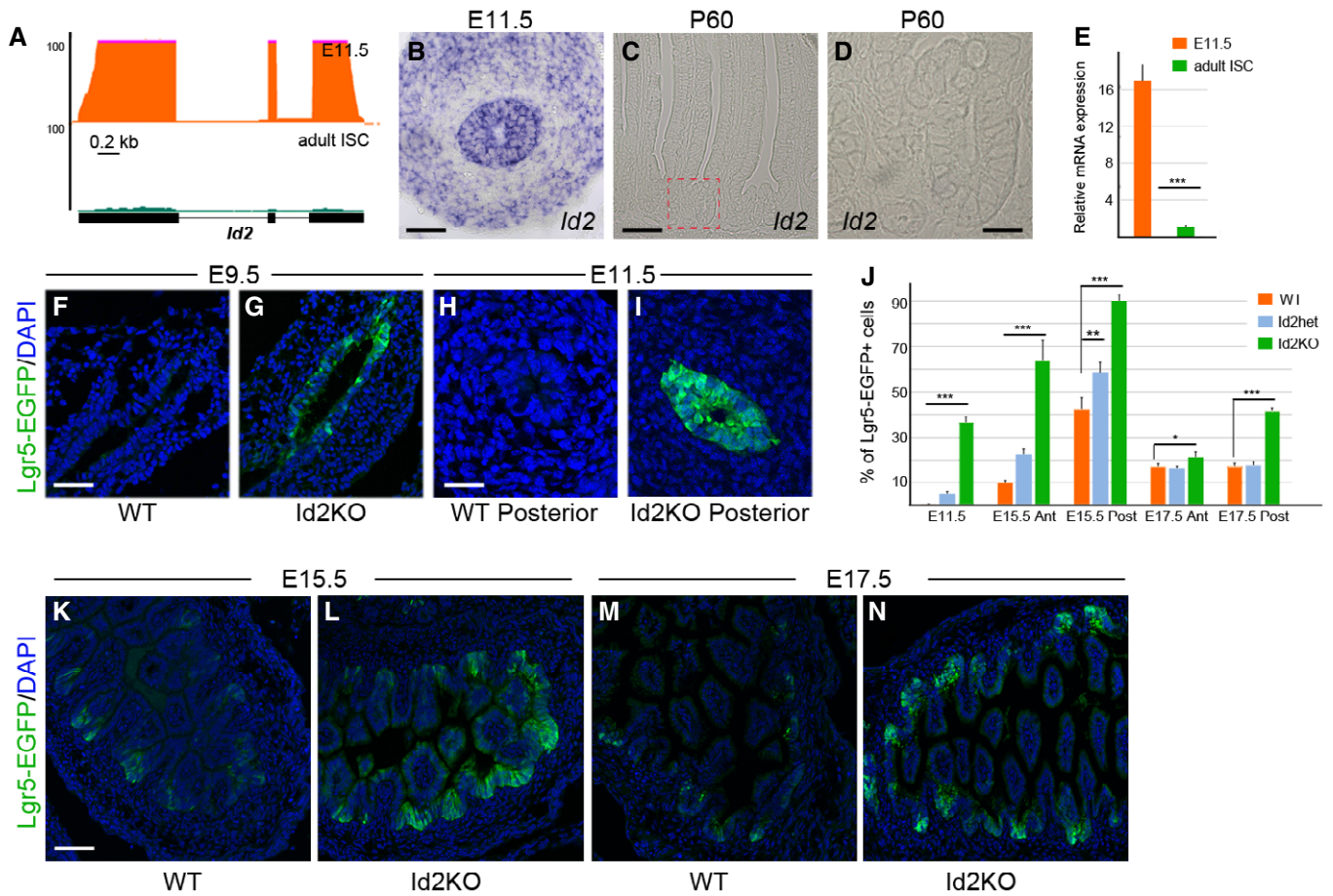


Figure 4. *Id2* regulates formation of Lgr5⁺ cells during embryogenesis.

A UCSC Genome Browser image of RNA-seq data demonstrating transcript profiles from embryonic small intestinal epithelium (orange) and the adult ISCs (green).
B–D Expression pattern of *Id2* in the embryonic small intestine at E11.5 (**B**) and in the adult intestinal epithelium (**C**, **D**) as revealed by RNA *in situ* hybridization.
E qRT-PCR analysis of *Id2* expression in embryonic (orange) and the adult ISCs (green) cells. *Epcam* expression was used as normalizing control. Error bars are \pm SD ($n = 3$). *** $P < 0.001$ by Student's *t*-test.
F–I Sections of EGFP-stained small intestine from *Id2KO:Lgr5^{EGFP-Cre-ERT}* and control *Lgr5^{EGFP-Cre-ERT}* embryos showing distribution of Lgr5⁺ cells (green) at E9.5 (**F**, **G**) and E11.5 (**H**, **I**) ($n = 3$ mice analysed).
J Quantification of Lgr5-EGFP⁺EpCAM⁺ cells from *Id2KO*, *Id2het* and control small intestinal epithelium at various developmental stages. Error bars are \pm SD, $n \geq 3$. *** $P < 0.001$, ** $P < 0.01$, * $P < 0.05$ by Student's *t*-test.
K–N Sections of EGFP-stained small intestine from *Id2KO:Lgr5^{EGFP-Cre-ERT}* and control *Lgr5^{EGFP-Cre-ERT}* embryos showing distribution of Lgr5⁺ cells at E15.5 (**K**, **L**) and E17.5 (**M**, **N**) ($n = 3$ mice analysed).

Data information: Scale bar: 30 μ m (**B**, **F**, **G**), 40 μ m (**C**) and 11 μ m (**D**, **H**, **I**), 300 μ m (**K–N**). See also Fig EV2.

the embryonic intestinal epithelium at E11.5 (Fig 5A, B and D). Significantly more genes (84%) were upregulated in *Id2KO*-Lgr5⁺EpCAM⁺ compared to *Id2KO*Lgr5⁻EpCAM⁺ cells (Fig 5A). 13.8% of the upregulated genes were shared between both Lgr5-positive and Lgr5-negative cells, many of which were cell cycle regulators, such as *Ccnb1*, *Cdk1*, *Cdc6*, *Plk1*, *Ccnd2*, *Cdc20* and *Aurkb* (Fig 5A). This indicates that *Id2* negatively controls cell cycle progression and proliferation during gut development. Expression of known ISCs markers, including *Smoc2* (over 100-fold), *Sox9*, *Pdgfra*, *Bmp7*, *Id1* and *Mecom*, was elevated in *Id2KO* epithelium regardless of Lgr5 expression (Fig 5A and D). However, *Lrig1*, *Prom1*, *Slc12a2*, *Sp5* and *Tnfrsf19/Troy* were specifically upregulated in *Id2KO*-Lgr5⁺EpCAM⁺ cells (Fig 5B).

Overall, 57 out of 381 genes (15%, $P < 10^{-28}$) upregulated specifically in *Id2KO*Lgr5⁺EpCAM⁺ at E11.5 overlapped with the wild-type, E13.5 embryonic Lgr5⁺ gene signature (Fig 5B), thus demonstrating that *Id2* negatively regulates not only the expression of the *Lgr5* gene but also the whole Wnt-dependent molecular network during intestinal development. Surprisingly, the expression of *Ascl2* was not activated in *Id2KO*Lgr5⁺EpCAM⁺ epithelium (Fig 5D), suggesting that in the absence of *Id2*, *Ascl2* is dispensable for the activation of the stem cell programme. Interestingly, we observed 10-fold induction in the expression of *Wnt6* and *Wnt11* specifically in *Id2KO*Lgr5⁺EpCAM⁺ (Fig 5B and D), implying that *Id2* negatively controls the activation Wnt signalling in the embryonic epithelium.

Among the 521 genes downregulated upon *Id2* inactivation, 229 (44%, $P < 10^{-27}$) were genes, which are downregulated in wild-type embryos as development proceeds from E11.5 to E13.5 (Fig 5C and D). On the other hand, we have not observed upregulation of the known differentiation markers, including *Fabp1* or *Fabp2* in mutant epithelium compared to wild type, suggesting that *Id2* prevents the precocious maturation of the early embryonic epithelium.

Id2 is also expressed in the intestinal mesenchyme at E11.5 (Fig 4B), and since *Id2* inactivation is not limited to the epithelium in our model system, the early specification of Lgr5⁺ cells could also be linked to defects in the surrounding mesenchyme. To address this issue, we have additionally isolated 250 EpCAM⁻ mesenchymal cells from both mutant and wild-type embryos and compared their transcriptomes (Fig EV2G and H). We have identified only 14 genes upregulated and 183 downregulated ($\log_2FC \geq 0.5$, FDR < 0.01, Datasets EV11 and EV12) in *Id2*KO mesenchymal cells. Gene ontology analysis of the downregulated transcripts identified a set of genes belonging to heme and

porphyrin biosynthesis, and erythrocytes development ($P < 10^{-10}$). This suggests that the transcriptional changes observed in the mutant mesenchyme are due to secondary effects such as a different number of embryonic erythrocytes (Ji et al, 2008). No changes in the expression of either Bmp/Tgf β or Wnt, or R-spondin ligands were observed between mutant and control mesenchyme (Appendix Fig S4A), suggesting that alterations in signalling from the mesenchyme are not the cause for the phenotype we observed in the epithelium. Therefore, we conclude that *Id2* likely functions in the epithelial cells to regulate the specification of Lgr5⁺ cells during embryogenesis.

Id2 negatively regulates Wnt/ β -catenin signalling

Multiple targets of Wnt signalling are ectopically expressed in Lgr5⁺ cells in *Id2*KO small intestine at E11.5. To assess whether elevated Wnt signalling is required for the precocious specification of Lgr5⁺ cells within the embryonic epithelium, we examined the expression

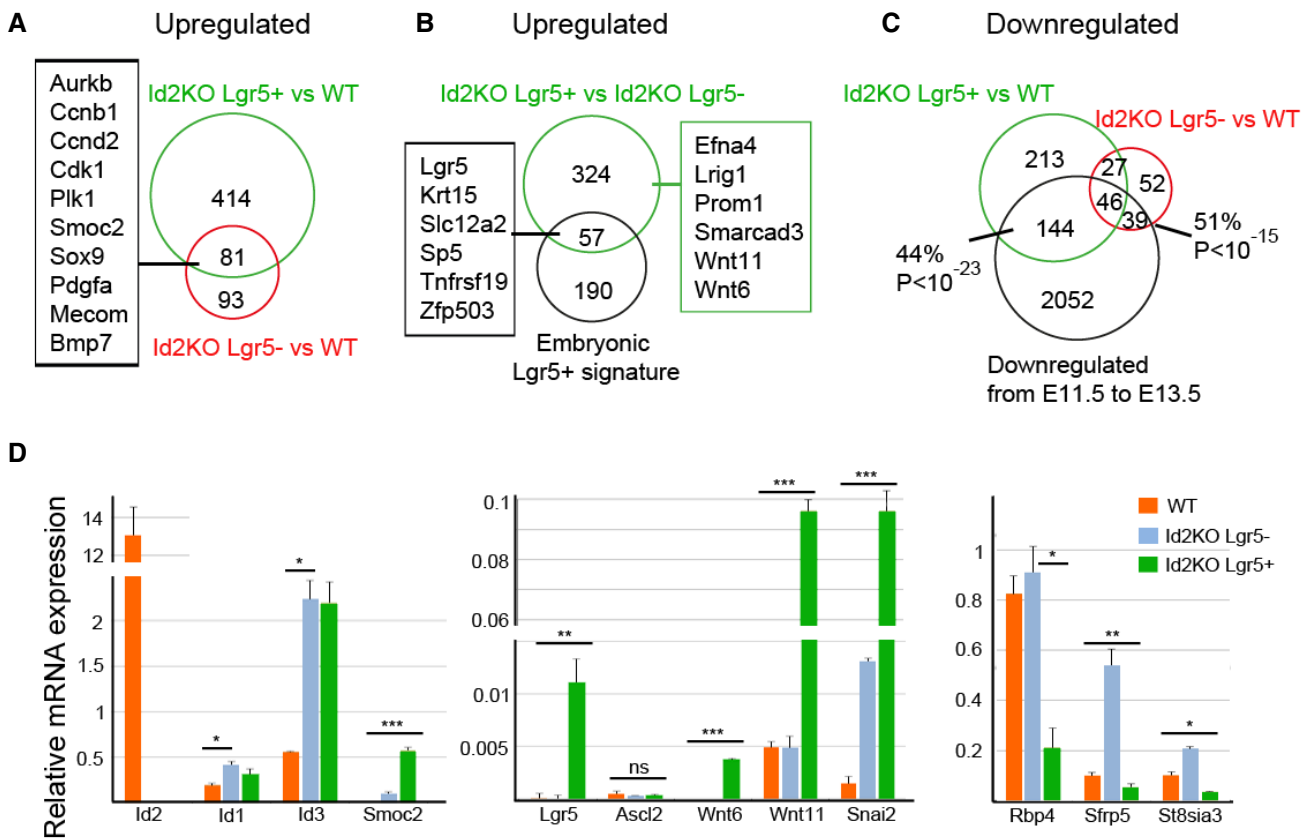


Figure 5. *Id2* is required for the repression of the ISCs signature genes during early embryogenesis.

A Venn diagram showing the overlap between genes upregulated in *Id2*KO Lgr5⁺ EpCAM⁺ (green) and *Id2*KO Lgr5⁻ EpCAM⁺ (red) cells compared to wild-type Lgr5⁻ EpCAM⁺ cells.
 B Venn diagram showing the overlap between genes upregulated in *Id2*KO Lgr5⁺ EpCAM⁺ (green) and embryonic Lgr5⁺ gene signature (black).
 C Venn diagram showing the overlap between genes downregulated in *Id2*KO Lgr5⁺ EpCAM⁺ (green), *Id2*KO Lgr5⁻ EpCAM⁺ (red) and E11.5 to E13.5 wild-type Lgr5⁻ EpCAM⁺ cells (black).
 D qRT-PCR analysis for selected genes differentially expressed in *Id2*KO Lgr5⁺ EpCAM⁺ (green) and *Id2*KO Lgr5⁻ EpCAM⁺ (blue) cells compared to control Lgr5⁻ EpCAM⁺ cells (orange). *Epcam* expression was used as normalizing control. Error bars are \pm SD ($n = 3$). *** $P < 0.001$, ** $P < 0.01$ and * $P < 0.05$ by Student's *t*-test.

Data information: See also Fig EV2 and Appendix Fig S4.

of Lgr5-EGFP following administration of the Wnt-C59 inhibitor, which prevents efficient secretion of Wnt ligands (Kabiri *et al*, 2014). Administration of Wnt-C59 at E13.5, E14.5 and E15.25 resulted in a dramatic loss (sixfold, $P < 0.01$) of Lgr5⁺ cells in wild-type embryos at E15.5 (Fig 6A and Appendix Fig S5A, B, D and E), indicating that Wnt signalling is required for Lgr5 expression during embryogenesis.

Loss of Lgr5⁺ cells was also observed in Id2KO embryos at E15.5 (Fig 6A and Appendix Fig S5A, C, D and F), yet to a lesser extent (up to threefold, $P < 0.01$). After Wnt-C59 treatment, most of Lgr5⁺ cells were detected in the posterior half of the small intestine in Id2KO embryos (Fig 6B–E). Notably, the residual Lgr5⁺ cells had lower expression of Lgr5-EGFP as revealed by FACS (Appendix Fig S5A–F) and anti-EGFP staining on sections (Fig 6B–E). The morphology of the small intestines from Id2KO or wild-type embryos treated with Wnt-C59 was similar to that from the control vehicle-treated embryos (Fig 6B–E). Specifically, villi formed normally and we did not observe increased apoptosis in the intestinal epithelium (data not shown). Importantly, administration of Wnt-C59 at E9.5 and E10.5 led to threefold ($P < 0.01$) reduction in the number of Lgr5⁺ cells in Id2KO embryos at E11.5 (Fig 6A and Appendix Fig S5G–I). Furthermore, qPCR analysis showed that not only Lgr5 but also other Id2KOLgr5⁺ signature genes were downregulated in Id2KO mutant epithelial cells upon Wnt-C59 treatment (Fig 6F). These data indicate that precocious activation of Wnt signalling is responsible for the premature specification of Lgr5⁺ cells in Id2 mutant intestinal epithelium.

Administration of Wnt-C59 had stronger effect on Lgr5⁺ cells from wild-type compared to Id2KO embryos (Fig 6A), suggesting that Id2 could have a repressive function in the transduction of Wnt/ β -catenin signalling downstream of Wnt ligands. Therefore, we tested the effect of Id2 overexpression on transcriptional activation of a β -catenin/Tcf-dependent luciferase reporter with six copies of Tcf-binding sites (TOPFlash). FOP reporter with mutated Tcf/Lef binding sites was used as a control for general transcriptional activity (Fig 6G). Overexpression of β -catenin resulted in significant activation of TOP reporter (up to 10-fold) in HEK 293T cells compared to control or FOP reporter (Fig 6G). Co-expression of Id2 decreased the TOP reporter activity in a dose-dependent manner (Fig 6G).

We then examined whether Id2 influence the levels of β -catenin protein. Consistent with the decrease in the transcriptional activity of the β -catenin-dependent reporter, we observed reduction in β -catenin protein levels in a dose-dependent manner upon overexpression of Id2 (Fig 6H). This decrease in β -catenin levels was dependent on the protein stability, since levels of β -catenin lacking its N-terminus, which is essential for phosphorylation and degradation of the protein, were less affected by Id2 overexpression (Fig 6H). Taken together, our data indicate that Id2 negatively regulates Wnt/ β -catenin-dependent transcription by affecting β -catenin protein stability.

Id2-deficient Lgr5⁺ progenitors have higher capacity to form organoids *ex vivo*

Transcriptional and FACS analyses revealed that Id2 restricts both the timing of Lgr5⁺ cell specification and their number. To evaluate whether Lgr5⁺ cells from Id2 mutant intestinal epithelium differ from wild-type cells by the expression levels of Lgr5 and the other

ISC signature genes, we isolated 250 Lgr5⁺EpCAM⁺ as well as Lgr5⁻EpCAM⁺ cells from Id2KO and control small intestines at E15.5, a time point when Lgr5⁺ cells are well defined and reside in the inter-villi compartment in wild-type embryos. qRT-PCR analysis showed that Lgr5, Smoc2 and Lrig1 were expressed at higher levels in posterior Id2KOLgr5⁺ compared to control cells (Fig 7A). Furthermore, Ccnb1 (cyclin b1), Ccnd2 (cyclin d2) and Trop2 (a marker of neoplastic transformation, Mustata *et al*, 2013; Zeng *et al*, 2016) were also expressed at higher levels in the posterior small intestine of Id2KO embryos compared to the controls (Fig 7A). On the other hand, Ascl2 was expressed at lower levels in Id2KOLgr5⁺ cells compared to wild-type control (Fig 7A). The expression of Snai2 was somewhat elevated, yet not significantly (Fig 7A).

To test the functional relevance of the gene expression changes caused by loss of Id2, we isolated by FACS Lgr5⁺EpCAM⁺ and Lgr5⁻EpCAM⁺ cells from Id2 mutant as well as wild-type embryonic intestines at E15.5 and assessed their capacity to form organoids *ex vivo* (Fig 7B). We applied the same culture conditions as were used for the adult Lgr5-EGFP^{high} ISCs (Sato *et al*, 2009), including essential growth factors R-spondin, Noggin, EGF and Rho kinase inhibitor. Two types of colonies were formed from E15.5 small intestinal epithelium: Lgr5⁺EpCAM⁺ cells give rise predominantly to organoids (Fig 7D and F; Fordham *et al*, 2013; Mustata *et al*, 2013), while Lgr5⁻EpCAM⁺ cells develop as spheroids (Fig 7E and G). Id2 ablation increased 3.7-fold the efficiency of organoid formation derived from Lgr5⁺EpCAM⁺ cells (Fig 7B and F). Moreover, both Id2KOLgr5⁻EpCAM⁺ and Id2KOLgr5⁺EpCAM⁺ cells gave rise to over 10 times more spheroids compared to the control (Figs 7B and G, and EV3A–F). Morphologically, Id2KO spheroids were 2–3 times larger compared to spheroids derived from the wild-type embryos (Fig 7E and G), which is consistent with an elevated expression of cell cycle promoting genes, including Ccnb1 and Ccnd2 (Fig 7A), in Id2 mutants. Further tests demonstrated that both Id2KO and wild-type colonies (both spheroids and organoids) required R-spondin, but not Noggin or EGF, for their survival (Fig EV3A–F).

qRT-PCR analysis showed that Lgr5, Axin2, Lrig1 and Smoc2 were expressed at higher levels in both Id2KO spheroids and organoids compared to the controls (Fig 7C), indicating that mutant cells gave rise to Lgr5⁺Axin2⁺ spheroids in *ex vivo* cultures. However, upon re-plating, Id2KO spheroids (derived from posterior Lgr5⁻EpCAM⁺ or Lgr5⁺EpCAM⁺ cells) readily formed organoids after the first passage. Moreover, Ascl2 was upregulated in Id2KO organoids compared to the controls (Fig 7C), whereas levels of Lyz1 (a marker for Paneth cells) were identical (Fig 7C), indicating that ISC signature genes are expressed at higher levels in Id2KO ISCs in culture. Strikingly, we detected strong activation of Snai2, Cnx43 and Trop2 in both Id2KO spheroids and organoids compared to the controls (Fig 7C). While Cnx43 and Trop2 were detected in wild-type spheroids (Fig 7C and Mustata *et al*, 2013), their levels were much lower compared to Id2KO spheroids or even organoids (Fig 7C), indicating that Id2KO cells form fast growing organoids expressing neoplastic markers. Consistent with *ex vivo* results, we observed high levels of nuclear Trop2 in Id2KO mutant intestines at P0 (Fig 7H and I). Of note, the presence of Trop2 receptor in the nucleus correlates with neoplastic transformation (Zeng *et al*, 2016).

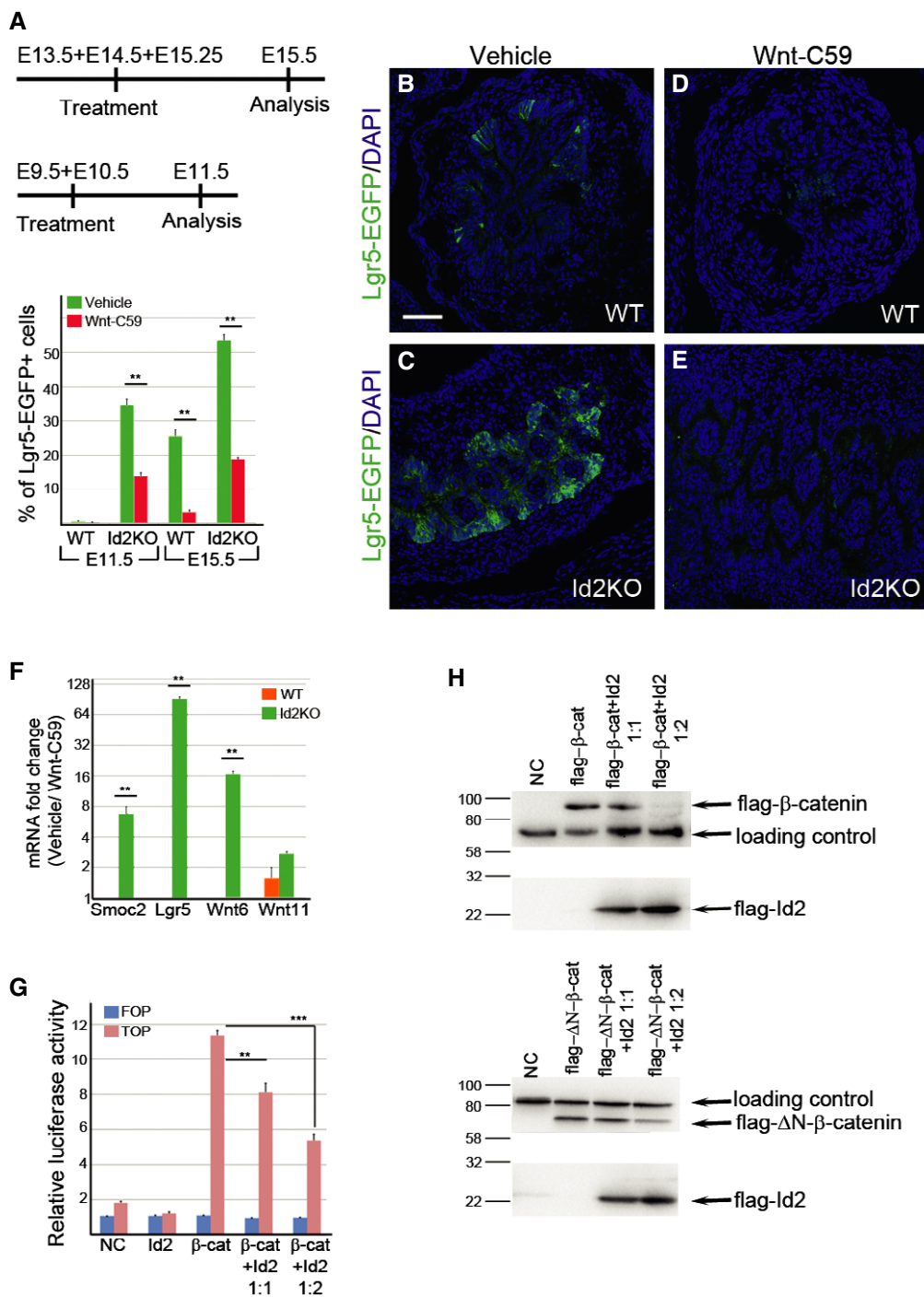


Figure 6. Id2 negatively controls Wnt/β-catenin signalling.

A FACS quantification of Lgr5⁺ cells in Id2KO and wild-type mice at E11.5 and E15.5 after administration of Wnt-C59 inhibitor (red) or vehicle (green). Error bars are ± SD (n = 3). ***P < 0.01 by Student's t-test.

B–E Sections of small intestines from *Lgr5^{EGFP-Cre-ERT}* (B, D) and *Id2KO:Lgr5^{EGFP-Cre-ERT}* embryos (C, E) at E15.5 stained with anti-GFP antibodies showing distribution of Lgr5⁺ cells (green) after administration of vehicle (B, C) or Wnt-C59 inhibitor (D, E). Scale bar: 100 μm.

F qRT-PCR analysis showing the expression of Id2KO Lgr5⁺ signature genes in Id2KO and wild-type intestinal epithelial cells at E11.5 after administration of Wnt-C59 inhibitor. Fold change (log2 scale) for vehicle over Wnt-C59-treated samples is shown. *Epcam* expression was used as normalizing control. Error bars are ± SEM (n = 2). ***P < 0.01 by Student's t-test.

G Id2 inhibits β-catenin-dependent transcription in a dose-dependent manner. Error bars are ± SD (n = 3). ***P < 0.001, **P < 0.01 by Student's t-test.

H Id2 expression decreases levels of β-catenin protein as revealed by Western blot analysis. HEK293T cells were transfected with plasmids expressing either flag-β-catenin or stabilized flag-ΔN-β-catenin with increasing amounts of plasmid expressing flag-Id2.

Data information: See also Appendix Fig S5.

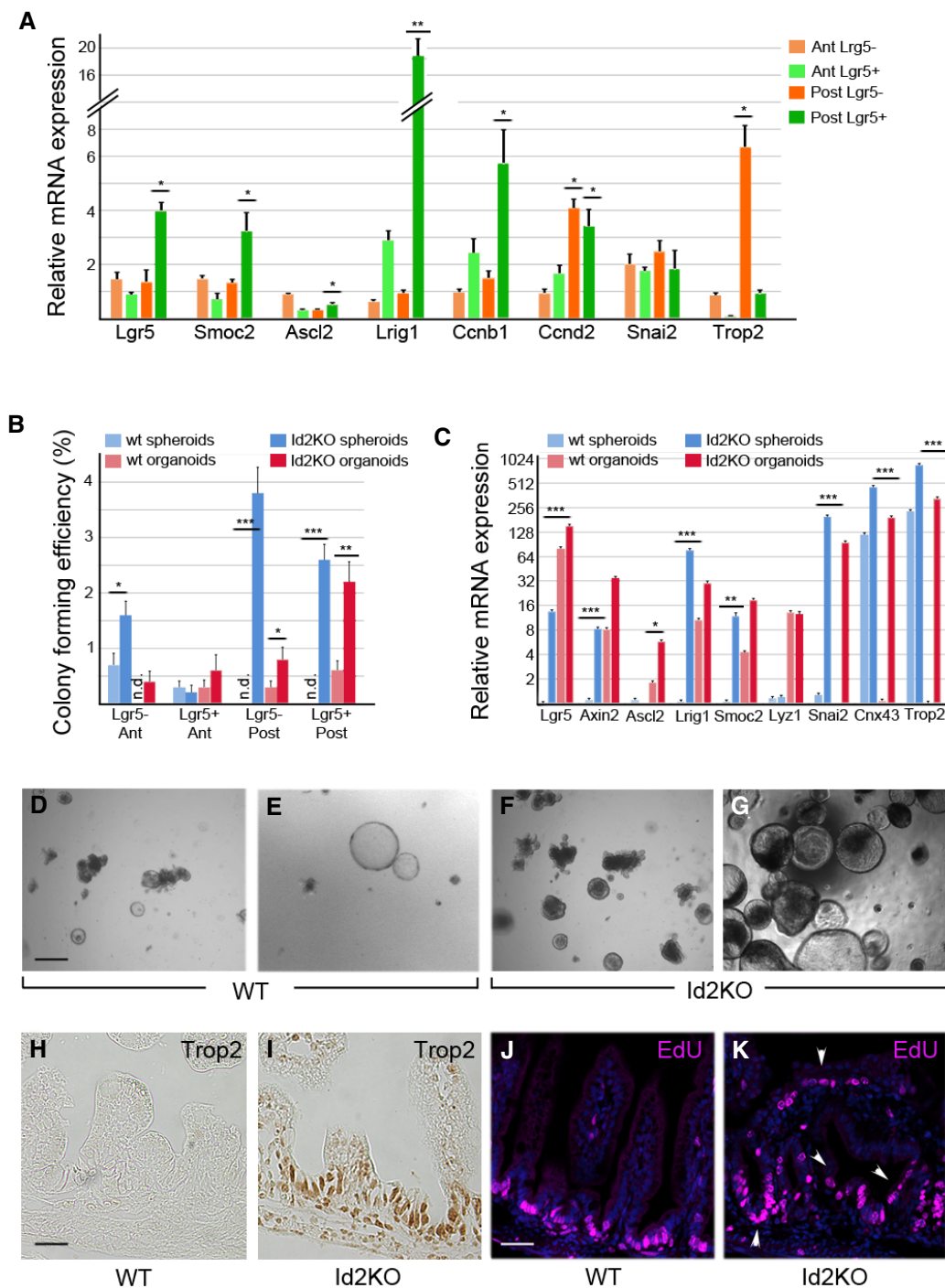


Figure 7. Id2 controls proliferation and differentiation of embryonic small intestinal epithelium.

A qRT-PCR analysis showing the expression of ISC signature, proliferation and neoplastic transformation marker genes in Id2KO and wild-type cells at E15.5. Fold change over wild-type values is shown. *Tbp* expression was used as normalizing control. Error bars are \pm SD ($n = 4$). $^{**}P < 0.01$ and $^{*}P < 0.05$ by Student's *t*-test.

B Colony-forming efficiency of wild-type and Id2KO cells isolated by FACS at E15.5. Error bars are \pm SD, $n = 4$. n.d. stands for not detected. $^{***}P < 0.001$, $^{**}P < 0.01$ and $^{*}P < 0.05$ by Student's *t*-test.

C qRT-PCR analysis for selected genes differentially expressed in Id2KO spheroids (dark blue) compared to wild-type spheroids (blue) and in Id2KO organoids (dark pink) compared to wild-type organoids (pink). *Tbp* expression was used as normalizing control. Error bars are \pm SD ($n = 3$). $^{***}P < 0.001$, $^{**}P < 0.01$ and $^{*}P < 0.05$ by Student's *t*-test.

D–G Representative images of primary organoids (**D**, **F**) and spheroids (**E**, **G**) at day 7 derived from wild-type and Id2KO cells at E15.5 ($n = 4$).

H–K Sections of small intestines from wild-type (**H**, **J**) and Id2KO (**I**, **K**) newborn mice stained with anti-Trop2 (**H**, **I**) or anti-EdU antibodies (**J**, **K**) showing distribution of Trop2⁺ and proliferating cells (pink, white arrowheads). Note the presence of nuclear Trop2 receptor in Id2KO inter-villi cells.

Data information: Scale bar: 2 mm (**D–G**), 30 μ m (**H**, **I**), 60 μ m (**J**, **K**). See also Fig EV3.

We further tested for proliferation rates in the intestinal epithelium of Id2KO and wild-type embryos both at E15.5 and P0. EdU⁺ proliferating cells were observed within hyperplastic lesions in Id2KO small intestines at P0 (Fig 7J and K). Yet, EdU⁺ cells were restricted to the inter-villi compartment in the non-hyperplastic regions of the small intestine in both mutant and control embryos (Fig EV3G and H), and their numbers were similar as measured by FACS (Fig EV3I). This is consistent with few hyperplastic events observed within Id2KO small intestines in adult mice. Together, our data demonstrate that *Id2* controls differentiation programmes in the embryonic intestinal epithelium by restricting the expression of genes promoting proliferation, Wnt signalling as well as epithelial to mesenchymal transition.

Precocious Lgr5⁺ cells are progenitors of the adult ISCs

To elucidate whether precociously specified Lgr5⁺ cells in Id2KO intestinal epithelium give rise to adult ISCs and contribute to the adult intestinal tissue, we performed lineage tracing analysis. For this purpose, we used *Id2*^{GFP} knock-in mice, in which the *Id2* gene is replaced by a *GFP* cassette, thus representing a null allele of *Id2* (Rawlins *et al*, 2009). Administration of tamoxifen at E11.5 to *Id2KO:Lgr5*^{EGFP-Cre-ERT}:*Rosa26*^{tdTomato} embryos resulted in expression of tdTomato in the adult small intestinal epithelium at P60 (Fig 8A–C). In contrast, tdTomato⁺ cells were not observed in *Lgr5*^{EGFP-Cre-ERT}:*Rosa26*^{tdTomato} small intestines at P60 (Fig 8B). Hence, precocious Lgr5⁺ cells labelled at E11.5 give rise to functional ISCs in adult Id2KO mice.

Consistent with the ectopic specification of Lgr5⁺ cells in the posterior half of the small intestine in Id2KO embryos, FACS analyses showed that only 0.1% of tdTomato⁺ cells could be detected in the anterior third of the small intestine in both *Lgr5*^{EGFP-Cre-ERT}:*Rosa26*^{tdTomato} and *Id2KO:Lgr5*^{EGFP-Cre-ERT}:*Rosa26*^{tdTomato} mice at P60 (Fig 8D, G and J). Furthermore, the percentage of Lgr5⁺ cells (either EGFP^{high} or EGFP^{low}) was identical in the anterior third of either Id2KO or control small intestines. Of note, in agreement with our RNA-sequencing data showing the absence of *Id2* expression in the adult ISCs, we did not detect expression of GFP in *Id2*^{GFP/GFP} adult intestinal epithelium either by immunostaining with anti-GFP antibody (Fig 8A) or by FACS (Fig 8D–F). The percentage of Lgr5⁺tdTomato⁺ (ISCs) cells progressively increased from the

middle (0.8%) to posterior (7.4%) thirds of the small intestine in *Id2KO:Lgr5*^{EGFP-Cre-ERT}:*Rosa26*^{tdTomato} mice at P60 (Fig 8E, F, H, I, K and L). Overall, 30% of Lgr5-EGFP^{high} cells were also tdTomato⁺ in the posterior third of the *Id2* mutant small intestine (Fig 8L). Moreover, larger number of Lgr5⁺ cells was detected in both the middle (12% versus 6% in wild type) and posterior (20% versus 5% in wild type) thirds of the small intestine in Id2KO compared to wild type at P60. These results indicate that loss of *Id2* results in a larger number of Lgr5⁺ cells in adult mice.

To further explore whether adult ISCs are affected by the loss of *Id2*, we performed RNA-sequencing of Id2KO and wild-type Lgr5⁺ ISCs from the anterior, middle and posterior parts of the small intestine. While ISC signature genes were expressed at overall similar levels in Id2KO and control cells, we observed significant differences in the mutant stem cells. Comparative analyses of transcriptomes revealed 200, 624 and 603 differentially expressed genes in anterior, middle and posterior ISCs, respectively (log₂FC ≥ 0.5, FDR < 0.01, Fig 8M and N, and Datasets EV13–EV18). GO term enrichment analysis revealed that most of the genes downregulated in Id2KO ISCs were associated with antigen processing and presentation ($P < 10^{-6}$; Fig 8M). Genes that were upregulated in the middle and posterior ISCs were enriched for the terms endoplasmic reticulum and metabolic process ($P < 10^{-6}$).

Interestingly, we have detected increased expression of several ISC signature genes (*Olfm4*, *Pdgfa*, *Sox9* and *Tnfrsf19*), genes expressed in both ISCs and transient amplifying cells (*Lrig1* and *Prom1*) as well as secretory progenitor markers (*Dll1* and *Spdef1*) in the middle Id2KO ISCs compared to wild type (Fig 8N). Furthermore, together with *Axin2* and *Prom1*, strong upregulation of secretory progenitor markers, including *Atoh1* (10-fold), *Spdef1* (10-fold), *Dll1*, *Dll4*, *Gfi1* and *Wnt3*, was observed in the posterior Id2KO ISCs compared to wild type (Fig 8N). Of note, we have performed RNA-sequencing analysis of either Lgr5⁺tdTomato⁺ or Lgr5⁺tdTomato⁻ Id2KO posterior ISCs. Comparative analysis of the transcriptomes did not reveal any difference in the gene expression between tdTomato⁺ and tdTomato⁻ ISCs, indicating that those cells are identical at P60. In summary, our data show that the precocious Lgr5⁺ Id2KO embryonic progenitors give rise to the adult ISCs, yet their numbers and transcriptional signatures differ from ISCs specified later during development in wild-type mice.

Figure 8. Precocious Id2KO Lgr5⁺ cells give rise to adult ISCs.

- A–C Sections of adult small intestines from *Id2*^{GFP/GFP}/*Rosa26*^{tdTomato} (A), *Lgr5*^{EGFP-Cre-ERT}/*Rosa26*^{tdTomato} (B) and *Id2*^{GFP/GFP}/*Lgr5*^{EGFP-Cre-ERT}/*Rosa26*^{tdTomato} mice (C) co-stained with EGFP antibody showing distribution of Lgr5:tdTomato⁺ progenies (red) and Lgr5-EGFP⁺ ISCs (green) at P60 after a single treatment with TAM at E11.5. Scale bar: 100 μm.
- D–L FACS plots showing tdTomato⁺EpCAM⁺ (red, Q1), Lgr5-EGFP⁺EpCAM⁺ (green, Q3) and double-positive Lgr5-EGFP⁺tdTomato⁺EpCAM⁺ (orange, Q2) cell populations in anterior (Ant), middle (Mid) and posterior (Post) parts of small intestine from *Id2*^{GFP/GFP}/*Rosa26*^{tdTomato} (D–F), *Lgr5*^{EGFP-Cre-ERT}/*Rosa26*^{tdTomato} (G–I) and *Id2*^{GFP/GFP}/*Lgr5*^{EGFP-Cre-ERT}/*Rosa26*^{tdTomato} (J–L) adult mice after a single treatment with TAM at E11.5 ($n = 2$). Cells in boxes represent Lgr5-EGFP^{high} ISCs, which were purified for further RNA-sequencing analysis.
- M Venn diagram showing the overlap between genes downregulated in anterior Id2KO Lgr5⁺ (green), middle Id2KO Lgr5⁺ (black) and posterior Id2KO Lgr5⁺ (red) ISCs compared to wild-type Lgr5⁺ ISCs. The genes downregulated in Id2KO ISCs from all three parts of the small intestine are enriched for GO term Antigen processing.
- N Venn diagram showing the overlap between genes upregulated in anterior Id2KO Lgr5⁺ (green), middle Id2KO Lgr5⁺ (black) and posterior Id2KO Lgr5⁺ (red) ISCs compared to wild-type Lgr5⁺ ISCs.
- O, P Functions of *Id2* during gut development. (O) In wild type, *Id2* prevents maturation and commitment of the small intestinal epithelial cells (yellow) towards Lgr5⁺ progenitors (green) from the time of gut tube formation (E9.5 till E13.5). Few Lgr5⁺ progenitors emerge at E13.5. The Lgr5⁺ cells reside within the inter-villi domain at E15.5 and at the bottom of the intestinal crypts in the adult gut. (P) In *Id2*-deficient intestinal epithelium, Lgr5⁺ cells emerge already at E9.5. Both Lgr5⁺ and Lgr5⁻ mutant cells display signs of precocious maturation, that is loss of the developmental stage-specific transcripts. The expression of Wnt/β-catenin targets and cell cycle promoting genes is elevated in *Id2* mutant epithelium. At E15.5, Lgr5⁺ cells represent a major population of the intestinal epithelium. Ectopic formation of Lgr5⁺ cells causes neoplastic transformation of the small intestinal epithelium (blue).

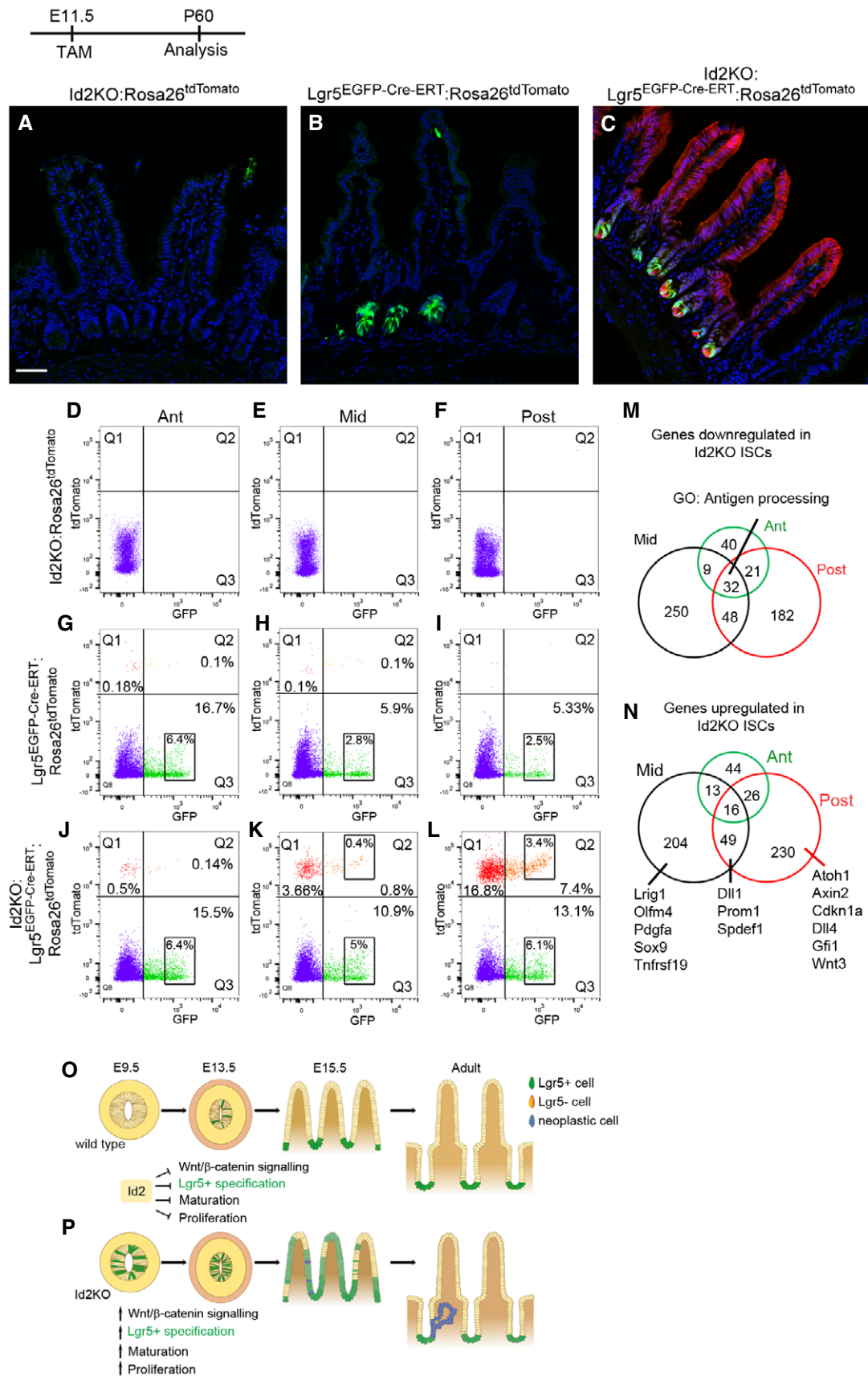


Figure 8.

Discussion

The adult ISCs are among the best-characterized tissue-specific stem cells, yet factors regulating the specification of their progenitors during development remained unknown. Here, we show that *Id2* is a key factor controlling the timing of Lgr5⁺ progenitor specification during embryogenesis (Fig 8O and P). Our cell fate mapping and transcriptome studies revealed that Lgr5⁺ progenitors emerge around E13.5 and represent only a minor fraction of the small intestinal epithelium in wild-type embryos. In contrast, in *Id2*-deficient embryos, Lgr5⁺ cells appear several days earlier and are much more abundant. Ectopic expression of Wnt ligands is required for the precocious activation of the Wnt/ β -catenin target genes and earlier specification of Lgr5⁺ progenitors in *Id2* mutant intestine. Moreover, *Id2* negatively regulates the transcription of Wnt/ β -catenin-dependent genes and prevents precocious differentiation of the embryonic intestinal epithelium into Lgr5⁺ progenitors by affecting the stability of β -catenin protein. The precocious *Id2*-deficient Lgr5⁺ embryonic progenitors give rise to adult ISCs. Yet, the number of *Id2* mutant Lgr5⁺ cells and their transcriptional signature differ from those in wild-type mice. We further demonstrate that in the absence of *Id2*, embryonic epithelial cells derived from Lgr5⁺ progenitors form Lgr5⁺ Axin2⁺ spheroids *ex vivo*, supporting an essential role for *Id2* in the correct specification of intestinal stem cells.

Our results support a model in which the early embryonic intestinal epithelium is heterogeneous at the molecular and functional levels. Using lineage tracing, FACS, transcriptional profiling and *in situ* hybridization analyses, we found that Lgr5⁺ progenitors appear around E13.5, prior to remodelling of the intestinal epithelium. Importantly, Lgr5⁺ cells at this stage of development represent only a small fraction of the small intestinal epithelium. The number of Lgr5⁺ cells and their progenitor potential increase at later stages (E15.5). We further show that only Lgr5⁺ progenitors display an intestinal stem cell signature, characterized by the expression of multiple Wnt-dependent target genes. In contrast, Lgr5-negative cells as well as the intestinal epithelial cells at earlier embryonic stages, prior to E13.5, differ significantly from the adult ISCs at the transcriptional level. Our data indicate that *Wnt5a* is the only *Wnt* expressed in the embryonic small intestine, both in the mesenchyme and in the epithelium, at E11.5. However, *Wnt5a* regulates gut morphogenesis independently from β -catenin pathway (Cervantes *et al*, 2009), further supporting our conclusion that early development and growth of the embryonic small intestinal epithelium occurs in the absence of Wnt/ β -catenin signalling. Moreover, loss of *Tcf7l2* or *β -catenin* affects proliferation of the progenitors only after E15.5 (Korinek *et al*, 1998; Chin *et al*, 2016) implying that at this stage of development Wnt signalling starts to play its important roles in intestinal morphogenesis. Consistent with genetic studies, we show that inhibition of Wnt signalling using Wnt-C59 results in dramatic decrease in Lgr5⁺ cells in the embryonic intestinal epithelium at E15.5. Altogether, our data are in striking contrast to the recent suggestion that the early embryonic gut is composed of a homogeneous population of Wnt signalling positive Lgr5⁺ progenitors resembling adult ISCs (Shyer *et al*, 2015).

Our results show that the loss of *Id2* leads to the formation of Lgr5⁺ cells in the intestinal epithelium of the primitive gut tube at E9.5. The precocious, ectopic Lgr5⁺ cells were abundant, comprising 30% of the intestinal epithelium in mutant embryos at E11.5.

RNA-sequencing analysis demonstrated that many genes defining the embryonic Lgr5⁺ progenitor signature were upregulated upon loss of *Id2*. Moreover, genes specifically expressed in the adult ISCs, such as *Lrig1* and *Prom1*, were also upregulated in Lgr5⁺ cells of *Id2* mutants at E11.5, suggesting that *Id2* inhibits maturation of the embryonic intestinal epithelium. Accordingly, genes encoding factors typical for the early embryonic epithelium were downregulated in *Id2*KO cells. Interestingly, a subset of the ISC signature genes as well as genes promoting cell proliferation were upregulated in all mutant epithelial cells regardless of *Lgr5* expression status, indicating that transcriptional programmes regulating cell cycle progression and Wnt signalling could be uncoupled in the embryonic intestinal epithelium.

Id2 function is required to prevent precocious activation of Wnt signalling in the embryonic intestinal epithelium. In our mutant model, *Id2* inactivation is not limited to the epithelium, and hence, the phenotype observed in *Id2*KO embryos might be linked to defects in the surrounding mesenchyme. We consider this possibility unlikely, since we found only minor changes in the mutant mesenchymal transcriptome. Most importantly, we did not observe changes in the expression of any known signalling molecule in the mutant mesenchyme.

Our RNA-sequencing data suggest that *Id2* could maintain an early intestinal endoderm state through the repression of *Wnt6* and *Wnt11*, which are specifically upregulated in Lgr5⁺ mutant cells. *Wnt6* and *Wnt11* are expressed during definitive endoderm formation (Krawetz & Kelly, 2008; Sinha *et al*, 2015) but absent in the embryonic intestinal epithelium once it is specified. Addition of *Wnt6* to *ex vivo* cultured intestinal organoids promotes their growth (Farin *et al*, 2012), implying that this Wnt ligand could activate transcription of β -catenin/Tcf7l2-dependent target genes in *Id2* mutant epithelium. Indeed, preventing *Wnt6* and/or *Wnt11* secretion using Wnt-C59 inhibitor resulted in a significant loss of Lgr5⁺ cells in *Id2* mutant intestinal epithelium at E11.5. Furthermore, our *in vitro* studies showed that *Id2* negatively regulates Wnt/ β -catenin-dependent transcription by affecting levels of β -catenin protein. Defining the precise molecular mechanisms underlying *Id2*-mediated degradation of β -catenin and repression of Wnt ligands will be the focus of future research.

At later stages, *Id2* mutant embryos showed a delay in differentiation of the intestinal epithelial cells as characterized by a dramatic decrease in the number of Lgr5-negative cells. *Id2* mutant cells, either Lgr5 negative or positive, when exposed to elevated Wnt and EGF stimuli in *ex vivo* culture, showed higher proliferation potential and preferentially formed less differentiated spheroid structures compared to Lgr5⁺ wild-type cells. Moreover, organoids derived from *Id2* mutant epithelium expressed higher levels of ISC signature genes as well as markers of neoplastic transformation, such as *Snai2* and *Trop2* compared to those from wild-type epithelium, supporting a role for *Id2* in a correct specification of intestinal epithelial cells during development. Accordingly, we detected the formation of neoplastic epithelium in *Id2* mutant neonatal intestine, as was previously reported (Russell *et al*, 2004).

Importantly, precocious Lgr5⁺ embryonic progenitors gave rise to the adult ISCs and contributed to the adult gut tissue. However, loss of *Id2* leads to four times increase in the number of Lgr5⁺ cells within the posterior small intestine compared to wild type in adult mice. Our RNA-sequencing data further revealed that mutant ISCs

have different transcriptional signature compared to wild type. While they expressed the same levels of ISC signature genes, such as *Lgr5* and *Ascl2*, mutant cells displayed higher levels of *Prom1* and *Axin2*, as well as genes belonging to secretory progenitor signature, including *Dll1*, *Dll4* and *Atoh1*. This suggests that although adult Lgr5⁺ ISCs could be specified from the precocious Id2-deficient Lgr5⁺ progenitors, these cells also express genes normally found in other cell types and might thus differ functionally from their wild-type counterparts, which could explain the formation of neoplastic lesions in Id2 mutant mice.

In summary, we identify Id2 as a key regulator of Lgr5⁺ progenitor specification during gut development. Our data showing that Id2 limits the number and proliferation of intestinal epithelial progenitors provide a better understanding of its function as a tumour suppressor. Our study highlights that precocious formation of Lgr5⁺ progenitors affects their transcriptional programmes and has important implications for the development of strategies for generating intestinal stem cells from pluripotent ES or iPS cells.

Materials and Methods

Mice

Lgr5^{EGFP-Cre-ERT}, *Id2^{Cre-ERT}*, *Id2^{GFP}*, *Prom1^{LacZ-Cre-ERT}*, *Rosa26^{tdTomato}* and *Rosa26^{lacZ}* mice were obtained from Jackson Laboratory. *Rosa26^{Cre-ERT}* mice were kindly provided by Ari Waisman, University of Mainz Medical School, Germany. Bl6/N and CD1 mice were from Charles Rivers. Tamoxifen (Sigma) was administered via oral gavage at 0.1 mg/g dam body weight. When P60 stage was required, newborn mice were fed by adoptive lactating CD1 females. EdU (Abcam) was administered at 25 µg/g dam body weight for 30 min. WntC59 (Tocris) was administered at 5 µg/g dam body weight. Mouse colonies were maintained in a certified animal facility in accordance with European guidelines. The experiments were approved by the local ethical committee.

Isolation of intestinal epithelial cells using flow cytometry

Cell staining and enrichment for isolation of adult ISCs were performed as described (Sato *et al*, 2009). Staining and isolation of embryonic intestinal epithelial populations were performed as described in the Appendix Supplementary Methods. Three to twenty independent biological replicates were used for each population. Fluorescence-activated cell sorting was performed using BD FACS Aria III SORP cell sorter (85 µm nozzle) and analysed using FlowJo software.

Transcript profiling and RNA-sequencing data analysis

For ultralow cell number RNA-sequencing, two hundred and fifty Id2KOLgr5-EGFP⁺EpCAM⁺, Id2KOLgr5-EGFP⁻EpCAM⁺, Lgr5-EGFP⁺EpCAM⁺, EpCAM⁺ embryonic intestinal cells and Lgr5-EGFP^{high} ISCs were isolated by FACS directly in 7 µl of lysis buffer (Clontech) supplemented with 5% RNase inhibitor and stored at -80°C. For each replicate, RNA was isolated from a single embryo. PolyA⁺ mRNA was used for cDNA synthesis using SMARTer v3.0 kit (Clontech) according to the manufacturer's instructions. Amplification

was performed for 15 cycles. After cDNA fragmentation (Covaris), libraries were prepared using Ovation Ultralow Library System (NuGEN) according to the manufacturer's instructions. Three independent FACS, cDNA synthesis, library preparations and sequencing experiments were performed. RNA-sequencing data analysis was performed as described in the Appendix Supplementary Methods. The sequencing data have been deposited in the NCBI Gene Expression Omnibus database.

Reverse transcription and quantitative PCR

For qRT-PCR, 10 ng of cDNA from Id2KOLgr5-EGFP⁺EpCAM⁺, Id2KOLgr5-EGFP⁻EpCAM⁺, Lgr5-EGFP⁺EpCAM⁺, EpCAM⁺ embryonic intestinal cells and Lgr5-EGFP^{high} ISCs was used. Expression changes were then normalized to *Tbp* and *Epcam*. PCR primers were designed using Primer Blast (<http://www.ncbi.nlm.nih.gov/tools/primer-blast/>) or qPCR Primers software from UCSC genome browser (<http://genome.ucsc.edu>). PCR was performed using SYBR green containing master mix kit (Applied Biosystems) with ViiATM 7 cyclor (Applied Biosystems). A mean quantity was calculated from triplicate reactions for each sample.

Ex vivo culture of intestinal organoids

Id2KOLgr5-EGFP⁺EpCAM⁺, Id2KOLgr5-EGFP⁻EpCAM⁺, Lgr5-EGFP⁺EpCAM⁺ and EpCAM⁺ intestinal cells were isolated from mouse embryos at E15.5 by FACS directly in 15 µl of advanced DMEM/F12 media containing B27-supplement (Gibco), non-essential amino acids, 2 mM L-glutamine, 15 mM HEPES and antibiotics and plated at a density of 500 cells per 30 µl of Matrigel drop (Invitrogen). Both cell culture medium and Matrigel were supplemented with growth factors (Sato *et al*, 2009), including 500 ng/ml human R-spondin1 (R&D Systems), 100 ng/ml Noggin (R&D Systems), 100 ng/ml EGF (R&D Systems) and 10 µg/ml Y-27632 inhibitor (R&D Systems). After 5 days in culture, organoids/spheroids were counted every day, imaged and collected for immunohistochemistry. Colony-forming efficiency was calculated by assessing organoid/spheroid formation 5–9 days after initiation of cultures. Images were acquired with Leica AF7000 microscope. At least three independent biological replicates were used for each population.

RNA in situ hybridization and histological techniques

RNA *in situ* hybridization on paraffin sections, β-galactosidase staining and immunohistochemistry of tissue sections and organoids were performed as described in the Appendix Supplementary Methods. At least three independent biological replicates were used for each experiment. Images were acquired with Leica DM2500, Leica AF7000 and Leica M205FA microscopes.

Data availability

The data sets supporting the conclusions of this article are available in the NCBI Gene Expression Omnibus repository (NCBI GEO: GSE90470).

Expanded View for this article is available online.

Acknowledgements

We thank J. Hartwig and I. Schaefer (Cytometry platform), M. Mendez-Lago, C-T. Han, C. Werner and H. Lukas (Genomics platform), S. Ritz and M. Hanulova (Microscopy platform) and P. Gusev for help; L. Fauk and K. Weiser for assistance with mouse breeding, A. Waisman for mice. We thank W. Birchmeier and J. Heuberger for advice; and T. Montavon for valuable comments on the manuscript. This work was funded by the Boehringer Ingelheim Foundation, the EU Marie Curie CIG program (PCIG12-GA-2012-333859 FaME) and the University of Mainz (NMFZ Nr 2013-22) to N.S.

Author contributions

LN, MN, MMD, BM and NS performed experiments and analysed the data. SS and NS performed analyses of RNA-sequencing data. NS designed the study and wrote the manuscript with inputs from LN.

Conflict of interest

The authors declare that they have no conflict of interest.

References

- Barker N, van Es JH, Kuipers J, Kujala P, van den Born M, Cozijnsen M, Haegerbarth A, Korving J, Begthel H, Peters PJ, Clevers H (2007) Identification of stem cells in small intestine and colon by marker gene Lgr5. *Nature* 449: 1003–1007
- Cervantes S, Yamaguchi TP, Hebrok M (2009) Wnt5a is essential for intestinal elongation in mice. *Dev Biol* 326: 285–294
- Chin AM, Tsai YH, Finkbeiner SR, Nagy MS, Walker EM, Ethen NJ, Williams BO, Battle MA, Spence JR (2016) A dynamic WNT/ β -CATENIN signaling environment leads to WNT-independent and WNT-dependent proliferation of embryonic intestinal progenitor cells. *Stem Cell Reports* 7: 826–839
- Clevers H, Loh KM, Nusse R (2014) Stem cell signaling. An integral program for tissue renewal and regeneration: Wnt signaling and stem cell control. *Science* 346: 1248012
- Dusing MR, Maier EA, Aronow BJ, Wiginton DA (2010) Onecut-2 knockout mice fail to thrive during early postnatal period and have altered patterns of gene expression in small intestine. *Physiol Genomics* 42: 115–125
- Farin HF, Van Es JH, Clevers H (2012) Redundant sources of Wnt regulate intestinal stem cells and promote formation of Paneth cells. *Gastroenterology* 143: 1518–1529
- Fevr T, Robine S, Louvard D, Huelsenken J (2007) Wnt/ β -catenin is essential for intestinal homeostasis and maintenance of intestinal stem cells. *Mol Cell Biol* 27: 7551–7559
- van der Flier LG, Haegerbarth A, Stange DE, van de Wetering M, Clevers H (2009b) OLFM4 is a robust marker for stem cells in human intestine and marks a subset of colorectal cancer cells. *Gastroenterology* 137: 15–17
- van der Flier LG, van Gijn ME, Hatzis P, Kujala P, Haegerbarth A, Stange DE, Begthel H, van den Born M, Guryev V, Oving I, van Es JH, Barker N, Peters PJ, van de Wetering M, Clevers H (2009a) Transcription factor achaete scute-like 2 controls intestinal stem cell fate. *Cell* 136: 903–912
- Fordham RP, Yui S, Hannan NR, Soendergaard C, Madgwick A, Schweiger PJ, Nielsen OH, Vallier L, Pedersen RA, Nakamura T, Watanabe M, Jensen KB (2013) Transplantation of expanded fetal intestinal progenitors contributes to colon regeneration after injury. *Cell Stem Cell* 13: 734–744
- García MI, Ghiani M, Lefort A, Libert F, Strollo S, Vassart G (2009) LGR5 deficiency deregulates Wnt signaling and leads to precocious Paneth cell differentiation in the fetal intestine. *Dev Biol* 331: 58–67
- Haramis AP, Begthel H, van den Born M, van Es J, Jonkheer S, Offerhaus GJ, Clevers H (2004) *De novo* crypt formation and juvenile polyposis on BMP inhibition in mouse intestine. *Science* 303: 1684–1686
- He XC, Zhang J, Tong WG, Tawfik O, Ross J, Scoville DH, Tian Q, Zeng X, He X, Wiedemann LM, Mishina Y, Li L (2004) BMP signaling inhibits intestinal stem cell self-renewal through suppression of Wnt- β -catenin signaling. *Nat Genet* 36: 1117–1121
- Ji M, Li H, Suh HC, Klarmann KD, Yokota Y, Keller JR (2008) Id2 intrinsically regulates lymphoid and erythroid development via interaction with different target proteins. *Blood* 112: 1068–1077
- Kabiri Z, Greicius G, Madan B, Biechele S, Zhong Z, Zaribafzadeh H, Edison, Aliyev J, Wu Y, Bunte R, Williams BO, Rossant J, Virshup DM (2014) Stroma provides an intestinal stem cell niche in the absence of epithelial Wnts. *Development* 141: 2206–2215
- Kim KA, Kakitani M, Zhao J, Oshima T, Tang T, Binnerts M, Liu Y, Boyle B, Park E, Emtage P, Funk WD, Tomizuka K (2005) Mitogenic influence of human R-spondin1 on the intestinal epithelium. *Science* 309: 1256–1259
- Kinzel B, Pikiolak M, Orsini V, Sprunger J, Isken A, Zietzling S, Desplanches M, Dubost V, Breustedt D, Valdez R, Liu D, Theil D, Müller M, Dietrich B, Bouwmeester T, Ruffner H, Tchorz JS (2014) Functional roles of Lgr4 and Lgr5 in embryonic gut, kidney and skin development in mice. *Dev Biol* 390: 181–190
- Kohlhoffer BM, Thompson CA, Walker EM, Battle MA (2016) GATA4 regulates epithelial cell proliferation to control intestinal growth and development in mice. *Cell Mol Gastroenterol Hepatol* 2: 189–209
- Korinek V, Barker N, Moerer P, van Donselaar E, Huls G, Peters PJ, Clevers H (1998) Depletion of epithelial stem-cell compartments in the small intestine of mice lacking Tcf-4. *Nat Genet* 19: 379–383
- Krawetz R, Kelly GM (2008) Wnt6 induces the specification and epithelialization of F9 embryonal carcinoma cells to primitive endoderm. *Cell Signal* 20: 506–517
- Lasorella A, Benezra R, Iavarone A (2014) The ID proteins: master regulators of cancer stem cells and tumour aggressiveness. *Nat Rev Cancer* 14: 77–91
- Matsuyama M, Aizawa S, Shimono A (2009) Sfrp controls apicobasal polarity and oriented cell division in developing gut epithelium. *PLoS Genet* 5: e1000427
- Muñoz J, Stange DE, Schepers AG, van de Wetering M, Koo BK, Itzkovitz S, Volckmann R, Kung KS, Koster J, Radulescu S, Myant K, Versteeg R, Sansom OJ, van Es JH, Barker N, van Oudenaarden A, Mohammed S, Heck AJ, Clevers H (2012) The Lgr5 intestinal stem cell signature: robust expression of proposed quiescent ‘+4’ cell markers. *EMBO J* 31: 3079–3091
- Mustata RC, Vasile G, Fernandez-Vallone V, Strollo S, Lefort A, Libert F, Monteyne D, Pérez-Morga D, Vassart G, Garcia MI (2013) Identification of Lgr5-independent spheroid-generating progenitors of the mouse fetal intestinal epithelium. *Cell Rep* 5: 421–432
- Powell AE, Wang Y, Li Y, Poulin EJ, Means AL, Washington MK, Higginbotham JN, Juchheim A, Prasad N, Levy SE, Guo Y, Shyr Y, Aronow BJ, Haigis KM, Franklin JL, Coffey RJ (2012) The pan-ErbB negative regulator Lrig1 is an intestinal stem cell marker that functions as a tumor suppressor. *Cell* 149: 146–158
- Rawlins EL, Clark CP, Xue Y, Hogan BL (2009) The Id2 + distal tip lung epithelium contains individual multipotent embryonic progenitor cells. *Development* 136: 3741–3745
- Russell RG, Lasorella A, Dettin LE, Iavarone A (2004) Id2 drives differentiation and suppresses tumor formation in the intestinal epithelium. *Cancer Res* 64: 7220–7225
- Sato T, Vries RG, Snippert HJ, van de Wetering M, Barker N, Stange DE, van Es JH, Abo A, Kujala P, Peters PJ, Clevers H (2009) Single Lgr5 stem cells

- build crypt-villus structures *in vitro* without a mesenchymal niche. *Nature* 459: 262–265
- Schuijers J, Junker JP, Mokry M, Hatzis P, Koo BK, Sasselli V, van der Flier LG, Cuppen E, van Oudenaarden A, Clevers H (2015) *Ascl2* acts as an R-spondin/Wnt-responsive switch to control stemness in intestinal crypts. *Cell Stem Cell* 16: 158–170
- Shibata H, Toyama K, Shioya H, Ito M, Hirota M, Hasegawa S, Matsumoto H, Takano H, Akiyama T, Toyoshima K, Kanamaru R, Kanegae Y, Saito I, Nakamura Y, Shiba K, Noda T (1997) Rapid colorectal adenoma formation initiated by conditional targeting of the *Apc* gene. *Science* 278: 120–123
- Shyer AE, Huycke TR, Lee C, Mahadevan L, Tabin CJ (2015) Bending gradients: how the intestinal stem cell gets its home. *Cell* 161: 569–580
- Sinha T, Lin L, Li D, Davis J, Evans S, Wynshaw-Boris A, Wang J (2015) Mapping the dynamic expression of *Wnt11* and the lineage contribution of *Wnt11*-expressing cells during early mouse development. *Dev Biol* 398: 177–192
- Sodir NM, Chen X, Park R, Nickel AE, Conti PS, Moats R, Bading JR, Shibata D, Laird PW (2006) *Smad3* deficiency promotes tumorigenesis in the distal colon of *ApcMin*⁺ mice. *Cancer Res* 66: 8430–8438
- Takaku K, Oshima M, Miyoshi H, Matsui M, Seldin MF, Taketo MM (1998) Intestinal tumorigenesis in compound mutant mice of both *Dpc4* (*Smad4*) and *Apc* genes. *Cell* 92: 645–656
- Walker EM, Thompson CA, Battle MA (2014) *GATA4* and *GATA6* regulate intestinal epithelial cytodifferentiation during development. *Dev Biol* 392: 283–294
- Wells JM, Spence JR (2014) How to make an intestine. *Development* 141: 752–760
- Whissell G, Montagni E, Martinelli P, Hernando-Momblona X, Sevillano M, Jung P, Cortina C, Calon A, Abuli A, Castells A, Castellvi-Bel S, Nacht AS, Sancho E, Stephan-Otto Attolini C, Vicent GP, Real FX, Batlle E (2014) The transcription factor *GATA6* enables self-renewal of colon adenoma stem cells by repressing BMP gene expression. *Nat Cell Biol* 16: 695–707
- Wong VW, Stange DE, Page ME, Buczaccki S, Wabik A, Itami S, van de Wetering M, Poulsom R, Wright NA, Trotter MW, Watt FM, Winton DJ, Clevers H, Jensen KB (2012) *Lrig1* controls intestinal stem-cell homeostasis by negative regulation of ErbB signalling. *Nat Cell Biol* 14: 401–408
- Zeng P, Chen MB, Zhou LN, Tang M, Liu CY, Lu PH (2016) Impact of *TROP2* expression on prognosis in solid tumors: a Systematic Review and Meta-analysis. *Sci Rep* 6: 33658